



**Assessing uncertainties of a geophysical approach to estimate surface  
fine particulate matter distributions from satellite observed aerosol  
optical depth**

5 Xiaomeng Jin<sup>1</sup>, Arlene M. Fiore<sup>1</sup>, Gabriele Curci<sup>2,3</sup>, Alexei Lyapustin<sup>4</sup>, Kevin Civerolo<sup>5</sup>, Michael  
Ku<sup>5</sup>, Aaron van Donkelaar<sup>6</sup>, Randall V. Martin<sup>6,7</sup>

1. Department of Earth and Environmental Sciences of Lamont-Doherty Earth Observatory  
and Columbia University, Palisades, NY, USA

2. Department of Physical and Chemical Sciences, University of L'Aquila, L'Aquila, Italy

10 3. CETEMPS, University of L'Aquila, L'Aquila, Italy

4. NASA Goddard Space Flight Center, MD, USA

5. New York State Department of Environmental Conservation, Albany, NY, USA

6. Department of Physics and Atmospheric Science, Dalhousie University, NS, Canada

7. Smithsonian Astrophysical Observatory, Harvard-Smithsonian Center for Astrophysics,

15 Cambridge, MA, USA



## Abstract

Health impact analyses are increasingly tapping the broad spatial coverage of satellite aerosol optical depth (AOD) products to estimate human exposure to fine particulate matter (PM<sub>2.5</sub>). We use a forward geophysical approach to derive ground-level PM<sub>2.5</sub> distributions from satellite AOD at 1 km<sup>2</sup> resolution for 2011 over the Northeast USA by applying relationships between surface PM<sub>2.5</sub> and column AOD (calculated offline from speciated mass distributions) from a regional air quality model (CMAQ; 12 × 12 km<sup>2</sup> horizontal resolution). Seasonal average satellite-derived PM<sub>2.5</sub> reveals more spatial detail and best captures observed surface PM<sub>2.5</sub> levels during summer. At the daily scale, however, satellite-derived PM<sub>2.5</sub> is not only subject to measurement uncertainties from satellite instruments, but more importantly, to uncertainties in the relationship between surface PM<sub>2.5</sub> and column AOD. Using 11 ground-based AOD measurements within 10 km of surface PM<sub>2.5</sub> monitors, we show that uncertainties in modeled PM<sub>2.5</sub>/AOD can explain more than 70% of the spatial and temporal variance in the total uncertainty in daily satellite-derived PM<sub>2.5</sub> evaluated at PM<sub>2.5</sub> monitors. This finding implies that a successful geophysical approach to deriving daily PM<sub>2.5</sub> from satellite AOD requires model skill at capturing day-to-day variations in PM<sub>2.5</sub>/AOD relationships. Overall, we estimate that uncertainties in the modeled PM<sub>2.5</sub>/AOD lead to an error of 11 μg/m<sup>3</sup> in daily satellite-derived PM<sub>2.5</sub>, and uncertainties in satellite AOD lead to an error of 8 μg/m<sup>3</sup>. Using multi-platform ground, airborne and radiosonde measurements, we show that uncertainties of modeled PM<sub>2.5</sub>/AOD are mainly driven by model uncertainties in aerosol column mass and speciation, while model uncertainties of relative humidity and aerosol vertical profile shape contribute some systematic biases. The parameterization of aerosol optical properties, which determines the mass-extinction efficiency, also contributes to random uncertainty, with the size distribution the largest source of uncertainty, and hygroscopicity of inorganic salt the second.



Future efforts to reduce uncertainty in geophysical approaches to derive surface  $PM_{2.5}$  from satellite AOD would thus benefit from improving model representation of aerosol vertical distribution and aerosol optical properties, to narrow uncertainty in satellite-derived  $PM_{2.5}$ .

*Keywords:*  $PM_{2.5}$ , aerosol optical depth, CMAQ, DISCOVER-AQ, aerosol size distribution,

5 aerosol hygroscopic growth.



## 1 Introduction

Exposure to ambient fine particulate matter (PM<sub>2.5</sub>) is estimated to cause more than 4 million attributable deaths worldwide in 2015 (Lim et al., 2016), and is associated with an increase in the risk of cardiovascular and respiratory disease (Dominici et al., 2006; Peng et al., 2009).

5 Evidence is emerging that exposure to PM<sub>2.5</sub> has adverse health effects even at low concentrations (Crouse et al., 2012; Shi et al., 2015). Early studies relied on the nearest ground-based monitors to estimate PM<sub>2.5</sub> exposure (e.g. Dockery et al., 1993; Laden et al., 2006), but lack of resolution of spatial and temporal gradients in population exposure may lead to substantial errors in health impact analyses.

10 Satellite remote sensing, which fills a spatial gap in ground-based networks, is playing an increasingly important role in PM<sub>2.5</sub> exposure assessment (Cohen et al., 2017; Jerrett et al., 2017). Aerosol optical depth (AOD), a measure of the sum of light extinction by aerosols within the atmospheric column, is retrieved from a number of satellite instruments. The Moderate Resolution Imaging Spectroradiometer (MODIS) on board Terra and Aqua has provided twice-daily global  
15 AOD data for nearly two decades, and the Multi-Angle Implementation of Atmospheric Correction (MAIAC) product has refined the spatial resolution retrieved from MODIS to 1 km (Lyapustin et al., 2011; 2012), offering the potential to reveal aerosol spatial variability within urban cores (Hu et al., 2014). A big challenge to inferring near-surface PM<sub>2.5</sub> from column AOD retrieved from  
20 satellite instruments is to describe accurately the non-linear and spatiotemporally varying relationship between PM<sub>2.5</sub> and AOD, which depends on aerosol chemical composition, vertical profiles, aerosol optical properties and the ambient environment (Griffin et al., 2012). Approaches to link satellite AOD with PM<sub>2.5</sub> exposures are often classified into two categories: statistical (e.g. Di et al., 2016; Hu et al., 2014; Kloog et al., 2014) and geophysical (e.g. van Donkelaar et al.,



2010; 2006). A two-stage process is also used with a geophysical approach followed by a statistical approach (e.g. van Donkelaar et al., 2015; de Hoogh et al., 2016; Shaddick et al., 2017).

Statistical approaches fit an optimized relationship between ground-based  $PM_{2.5}$  and satellite AOD along with other predictors (e.g. land use, meteorology, traffic density etc.) using  
5 methods such as multiple linear regression (e.g. Gupta and Christopher, 2009; Lee et al., 2016), geographic regression (Hu et al., 2014), generalized additive models (e.g. Kloog et al., 2014), or machine learning (Di et al., 2016). In regions with high monitor density, the statistical methods generally agree better with ground-based observations than  $PM_{2.5}$  derived with geophysical approach, but statistical methods rely on the availability of ground-based monitors to train the  
10 statistical model, and are thus limited to regions with dense monitoring networks.

The geophysical approach that has been applied to AOD is a process-based forward approach that uses chemical transport models to explicitly simulate the spatially and temporally varying relationship between column AOD and  $PM_{2.5}$  (van Donkelaar et al., 2006). The satellite-derived  $PM_{2.5}$  is calculated by taking the product of satellite AOD with the modeled ratio of  $PM_{2.5}$   
15 to AOD (van Donkelaar et al., 2006):

$$PM_{2.5_{sat}} = AOD_{sat} \times \frac{PM_{2.5_{model}}}{AOD_{model}} \quad (1)$$

This geophysical approach has the advantage of broad spatial coverage that is not limited by the availability of *in-situ* measurements (van Donkelaar et al., 2006), and thus has been integral for studying the global burden of disease attributable to ambient air pollution (Cohen et al., 2017).  
20 Van Donkelaar et al. (2010) estimate global annual average  $PM_{2.5}$  using AOD observed from both MODIS and MISR (Multiangle Imaging Spectroradiometer) by  $PM_{2.5}$ -AOD relationships from a global chemical transport model (GEOS-Chem). They estimate an overall uncertainty of around



25% for annual average satellite-derived  $PM_{2.5}$ , but the uncertainty of the geophysical approach at short-time scale is expected to be larger (van Donkelaar et al., 2012).

The overall uncertainty in deriving surface  $PM_{2.5}$  with the geophysical approach consists of uncertainty in the satellite AOD as well as the modeled  $PM_{2.5}/AOD$ . First, satellite observations  
5 of AOD are subject to uncertainties due to the viewing geometry, the presence of clouds and snow, and choices involved in modeling optical aerosol and surface properties (Superczynski et al., 2017; Toth et al., 2014). Second, since the relationship between  $PM_{2.5}$  and AOD is non-linear and multivariate, modeled  $PM_{2.5}/AOD$  is subject to model uncertainties in aerosol vertical distributions, aerosol speciation and the ambient environment. Third, even if a model simulates accurately the  
10 aerosol mass distribution, calculating AOD in models generally requires assumptions regarding the aerosol size distribution, aerosol species density, refractive index and hygroscopic growth factors, all of which are sources of uncertainties (Curci et al., 2015). The ability of a particle to scatter and absorb light largely depends on its size, which varies significantly in nature (Stanier et al., 2004). As resolving the size distribution is computationally expensive (Adams, 2002), aerosols  
15 are typically assumed to follow a certain distribution (e.g. log-normal), which can introduce error. Moreover, aerosol water uptake (hygroscopicity) affects the aerosol size and optical properties, but the representation of hygroscopic factors in models varies considerably by study (Chin et al., 2002; Curci et al., 2015; Drury et al., 2010). The hygroscopic growth factor for organic carbon (OC) is especially uncertain, varying considerably by organic species, and is poorly represented in models  
20 (Ming et al., 2005; Jimenez et al., 2009; Latimer and Martin, 2018). The impacts of these uncertainties on aerosol radiative forcing have been studied extensively in literature, but their impacts on deriving surface  $PM_{2.5}$  from satellite-based column AOD have not yet been quantified.



Here, we estimate  $PM_{2.5}$  distributions over the Northeast USA for 2011 using a geophysical approach that combines MAIAC AOD data with modeled  $PM_{2.5}$ /AOD relationships simulated with a regional air quality model (CMAQ). Compared to the global GEOS-Chem model used by van Donkelaar et al. (2016), CMAQ has finer spatial resolution ( $12 \times 12 \text{ km}^2$ ) and a locally refined emission inventory (see Sect. 2.2). We use an ensemble of surface (AQS, AERONET, IMPROVE, CSN), aircraft (DISCOVER-AQ) and radiosonde (IGRA) measurements to evaluate different sources of uncertainties in satellite-derived  $PM_{2.5}$ , especially at daily scale. To evaluate the sensitivities of satellite-derived  $PM_{2.5}$  to the parameterization of aerosol optical properties, we conduct a series of sensitivity tests in an offline AOD calculation package (FlexAOD). The overarching goal of the comprehensive uncertainty analysis is to assess the relative importance of each uncertain factor, thereby advancing the process-level understanding of the relationship between satellite AOD and surface  $PM_{2.5}$  air quality.

## 2 Data and methods

### 2.1 Satellite AOD

We use the high-resolution (1 km) daily AOD products retrieved from the MODIS instruments onboard Terra and Aqua satellites with the new MAIAC algorithm that is based on time series analysis and image processing techniques (Lyapustin et al., 2011; 2018). The spatial resolution of MAIAC (1 km) is finer than the conventional MODIS Dark Target and Deep Blue AOD products. The MAIAC algorithm improved upon the earlier Dark Target retrieval algorithm (MOD04) by explicitly including bi-directional reflectance (rather than the parameterized Dark Target approach), which improves accuracy over brighter surfaces, with similar accuracy over dark and vegetated surfaces (Lyapustin et al., 2011).



Using the quality flags provided, we filtered out pixels with or adjacent to cloud, snow or ice. We follow the approach of Hu et al. (2014) to combine daily MAIAC AOD from Terra (overpasses around 10:30 AM local time) and Aqua (overpasses around 1:30 PM local time). For the pixels where both Terra and Aqua have valid data, we take the average to reflect the mean daytime AOD. For pixels where only one instrument has valid data, AOD may be biased accordingly towards morning or afternoon conditions. We find, on average, Terra-MAIAC AOD is higher than Aqua-MAIAC AOD by 0.005 (about 5% of the annual average AOD) over the Northeast USA in 2011, reflecting diurnal variations of AOD (Green et al., 2012) and potential calibration differences (Levy et al., 2018). To account for these differences, we fit two linear equations ( $R = 0.87$ ) between Terra-MAIAC ( $AOD_T$ ) and Aqua-MAIAC AOD ( $AOD_A$ ):

$$\widehat{AOD}_T = 0.84AOD_A + 0.019 \quad (2)$$

$$\widehat{AOD}_A = 0.88AOD_T + 0.005 \quad (3)$$

We use Eq. (2) and (3) to predict the AOD from the other instrument when one of them is missing, and then take the average. We find little seasonal variation in the linear relationship.

## 2.2 CMAQ model

The Community Multiscale Air Quality Modeling System (CMAQ) is a regional multipollutant air quality model developed and maintained by the U.S. Environmental Protection Agency (EPA). We use the CMAQ (v5.0.2) model simulations for 2011 conducted at New York State Department of Environmental Conservation (NYSDEC) for air quality planning purposes. The simulations are conducted for the eastern USA with 12 km horizontal resolution and 35 vertical layers extending up to 50 hPa. The meteorological fields to drive CMAQ are provided by annual Weather Research and Forecast (WRF) v3.4 model simulations over continental United States. Chemical boundary conditions are from the GEOS-Chem ( $2^\circ \times 2.5^\circ$ ) global chemical





transport model (Bey et al., 2001, version 8) generated by EPA. The emission inventory is based on the 2011 National Emission Inventory (NEI) and processed through the Sparse Matrix Operator Kernel Emissions (SMOKE; (Houyoux et al., 2000)). Biogenic emissions are generated with the Biogenic Emissions Inventory System (BEIS) v3.61 (Pierce et al., 2002). Prescribed burning and wildfire emissions are computed using the SmartFire 2 (Raffuse et al., 2009). Mobile emissions are produced from the EPA's MOTO Vehicle Emission Simulator (MOVES) 2014a (US EPA, MOVES2014a). The gas-phase chemical mechanism is CB05, and the aerosol module is AERO6. Appel et al. (2013; 2017) provide details on the calculation of total PM<sub>2.5</sub> mass and speciated aerosol mass, as well as model evaluation.

### 2.3 Offline AOD calculation

We calculate hourly AOD from the CMAQ model (AOD<sub>CMAQ</sub>) offline from the archived hourly, three-dimensional, speciated aerosol (i.e. sulfate, nitrate, ammonium, black carbon, organic carbon, sea salt, soil dust) distribution and meteorological fields (i.e. relative humidity, thereafter RH) using the Flexible Aerosol Optical Depth (FlexAOD) post-processing tool. FlexAOD was originally developed to calculate aerosol optical properties for the GEOS-Chem model. It is based on the NASA Codes for Computation of Bidirectional Reflectance of Flat Particulate Layers and Rough Surfaces (Mishchenko et al., 1999). We adapt FlexAOD to CMAQ by matching the aerosol speciation with GEOS-Chem based on Appel et al. (2013). Under the assumption of spherical particles, aerosol optical properties are calculated based on Mie theory. Given size distributions for each aerosol species, aerosol light extinction ( $EXT_l$ ) at a given model layer is calculated as follows (Curci, 2012):

$$EXT_l = \sum_{i=1}^N \frac{3}{4} \frac{Q_{e,dry,i} f_{RH,l,i}}{r_{e,dry,i} \rho_i} M_{i,l} \quad (4)$$



where  $i$  refers to the species,  $N$  is the number of aerosol species ( $N = 5$ : sulfate-nitrate-ammonium (SNA), OC, black carbon (BC), dust, sea salt),  $\overline{Q_{e,dry,i}}$  is the Mie extinction efficiency of species  $i$  averaged over the dry size distribution,  $f_{RH,i}$  is the hygroscopic growth factor of species  $i$  at given  $RH$ ,  $\rho_i$  is aerosol density of species  $i$ ,  $M_{i,l}$  is the aerosol mass of species  $i$  at layer  $l$ , and

5  $r_{e,dry,i}$  is the dry effective radius.  $AOD_{CMAQ}$  is then calculated as the vertical integral of  $EXT_l$  across all model layers:

$$AOD_{CMAQ} = \int_{l=1}^L EXT_l dz \quad (5)$$

We use the recommended values of Drury et al. (2010) for aerosol density. The refractive index ( $m$ ) in the default run is adapted from the Optical Properties of Aerosols and Clouds (OPAC) database (Hess et al., 1998). As CMAQ does not explicitly simulate the size distribution of aerosols,

10 we assume log-normal distributions for all species except for dust (assumed to be a gamma distribution). The effective radius ( $r_e$ ), or the area-weighted mean radius of log-normal size distribution can be derived as:

$$r_{e,dry,i} = r_0 e^{\left(\frac{5}{2} \ln^2 \sigma_g\right)} \quad (6)$$

15 where  $r_0$  is the specific modal radius,  $\sigma_g$  is the geometric standard deviation. For the aerosol size distribution and density, we follow the recommended values of Drury et al. (2010) in the default run. We apply the single parameter  $\kappa$  to represent the hygroscopic growth of SNA and organic carbon, which is developed by Petters and Kreidenweis (2007) based on the  $\kappa$ -Kohler theory, and it is the most commonly accepted function in the literature (Brock et al., 2016; Snider 2016). The

20 hygroscopic growth factor can be simplified as a function of parameter  $\kappa$  and  $RH$  (Snider et al., 2016):

$$f(RH) = \left(1 + \kappa \frac{RH}{100 - RH}\right)^{1/3} \quad (7)$$



Koehler et al. (2006) suggest  $\kappa$  for SNA ( $\kappa_{\text{SNA}}$ ) ranges from 0.33 to 0.72, with a mean of 0.53. The hygroscopic growth factor of organic carbon ( $\kappa_{\text{OC}}$ ) varies with species and is correlated with the age of organics (Duplissy et al., 2011). Duplissy et al. (2011) and Jimenez et al. (2009) suggest  $\kappa$  for organic carbon typically ranges from 0 to 0.2. We apply  $\kappa_{\text{SNA}} = 0.53$ , and  $\kappa_{\text{OC}} = 0.1$  to represent  
5 the hygroscopic growths of SNA and OC. For black carbon and sea salt, we apply the hygroscopic growth factors reported in Chin et al. (2002). In addition to the default values, we test the sensitivities of the derived  $\text{PM}_{2.5}$  to uncertainties in aerosol optical property parameterization by varying each parameter using values reported in the literature, as specified in Table 1.

#### 2.4 Ground-based observations

10 AEROSOL ROBOTIC NETWORK (AERONET) is a federated instrument network that provides ground-based information about aerosols including AOD, which is derived from sun photometer measurements of direct solar radiation (Holben et al., 1998). We use Level-2 (cloud screened and quality assured) daily average data from 13 sites over the Northeast USA. We also include  
15 observed AOD from the Distributed Regional Aerosol Gridded Observation Networks (DRAGON)-USA 2011 field campaign, co-located with the DISCOVER-AQ aircraft campaign. The DRAGON campaign provides extensive sun photometer measurements of AOD at 38 sites along the flight path of DISCOVER-AQ from July 1 to August 15, 2011, which were incorporated into the AERONET database. To allow direct comparison with  $\text{AOD}_{\text{MAIAC}}$  and  $\text{AOD}_{\text{CMAQ}}$ ,  
20 AERONET AOD measurements at 0.44  $\mu\text{m}$  and 0.675  $\mu\text{m}$  were interpolated to 0.55  $\mu\text{m}$  using the Angstrom exponent (the first derivative of AOD with wavelength, on a logarithmic scale) provided (0.44 - 0.675  $\mu\text{m}$ ).

We use ground-based measurements of daily 24-hour average  $\text{PM}_{2.5}$  from 152 EPA Air Quality System (AQS) sites. Of the 152 sites, 13 sites have AERONET sites within 10 km (about



the resolution of CMAQ). We consider these 13 sites as “co-located” and use them to evaluate uncertainties in modeled  $PM_{2.5}$ /AOD relationships. We also use AQS aerosol speciation data at 54 sites which include the Chemical Speciation Network (CSN) and the Interagency Monitoring of Protected Visual Environments (IMPROVE) visibility monitoring network.

5 To evaluate the modeled vertical profile of ambient RH, we use ground-based soundings from 6 radiosonde sites over the Northeast USA. Aggregated daily data at 0:00 and 12:00 UTC are acquired from NOAA’s Integrated Global Radiosonde Archive (IGRA), and modeled vertical profiles are sampled concurrently with radiosonde observations. We use the RH data calculated from vapor pressure, saturation vapor pressure and ambient air pressure (Durre and Yin, 2008).

## 10 2.5 NASA DISCOVER-AQ 2011 Field Campaign

The NASA DISCOVER-AQ (Deriving Information on Surface conditions from Column and Vertically Resolved Observations Relevant for Air Quality) aircraft campaign over Baltimore-Washington, D.C. in July 2011 provides extensive, systematic, concurrent measurements of aerosol chemical, optical, and microscopic properties. The NASA P-3B aircraft performed 14  
15 flights which include 247 profiles (typically ranging from 0.4 to 3.2 km) over six DRAGON sites during the Baltimore-Maryland campaign in July 2011 (Crumeyrolle et al., 2014). In this study, we use the simultaneous measurements of aerosol composition (SNA, OC, BC), scattering, absorption, and extinction coefficients at dry ( $RH < 40\%$ ), ambient and wet ( $RH > 80\%$ ) environments. To reduce the random uncertainties of individual observations and to allow direct  
20 comparison with CMAQ and ground-observations, we aggregate the daily aircraft profiles horizontally to six locations corresponding to the six sites, and vertically to CMAQ model layers, and then sample CMAQ modeled values consistently with observations.



### 3 Results and Discussion

#### 3.1 Deriving surface $PM_{2.5}$ from satellite observations

We derive satellite-based  $PM_{2.5}$  (thereafter  $PM_{2.5\_MAIAC}$ ) over the Northeast USA for 2011 by taking the product of daily average CMAQ modeled  $PM_{2.5}/AOD$  relationships ( $PM_{2.5\_CMAQ}/AOD_{CMAQ}$ ) with MAIAC AOD ( $AOD_{MAIAC}$ , Eq. (1)). The unconstrained  $PM_{2.5}$  estimates are independent of surface observations. As  $PM_{2.5\_MAIAC}$  is determined as the product of observed  $AOD_{MAIAC}$  and modeled  $PM_{2.5\_CMAQ}/AOD_{CMAQ}$ , the spatial patterns of  $PM_{2.5\_MAIAC}$  will be affected by the spatial variations of both  $AOD_{MAIAC}$  and  $PM_{2.5\_CMAQ}/AOD_{CMAQ}$ . Fig. 1a) shows the summertime average (JJA)  $AOD_{MAIAC}$  at 1km resolution overlaid with AERONET observed AOD. While we find high AOD over some populated urban areas such as New York City (NYC), high  $AOD_{MAIAC}$  is also found over central New York State (NYS), away from the major anthropogenic sources. In CMAQ, while high  $PM_{2.5\_CMAQ}$  are located at regions with major anthropogenic sources such as NYC region,  $AOD_{CMAQ}$  shows a latitudinal dependence with higher AOD in low latitudes, which is due to 1) relatively high emissions of aerosol and its precursors from anthropogenic and biogenic sources over MD, PA and NYC; and 2) latitudinal variations of RH that affect aerosol hygroscopic growth. The modeled  $PM_{2.5\_CMAQ}/AOD_{CMAQ}$  varies spatially with standard deviation (SD) being  $45 \mu\text{g}/\text{m}^3$  per unit of AOD, which is mainly driven by the spatial variations of  $PM_{2.5\_CMAQ}$  ( $R = 0.86$ ). We find the overall spatial pattern of satellite-derived  $PM_{2.5}$  is more correlated with modeled  $PM_{2.5\_CMAQ}/AOD_{CMAQ}$  ( $R = 0.97$ ) than observed  $AOD_{MAIAC}$  ( $R = 0.8$ ), suggesting that the large-scale spatial variability is determined largely by the model rather than by the satellite observations at least under our framework for the Northeast USA in summer. At smaller scales, over which we assume the spatial variability of  $PM_{2.5}/AOD$  is



homogenous, incorporating fine-resolution satellite data reveals stronger spatial gradients (e.g., enhancements along industrial corridors) than  $PM_{2.5\_CMAQ}$  (Fig. 1b).

Besides improving the spatial resolution, satellite-derived  $PM_{2.5}$  can correct model summertime biases in  $PM_{2.5}$ . Evaluating model with observed AOD from AERONET and  $PM_{2.5}$  from AQS, we find an overall underestimate in both  $AOD_{CMAQ}$  (Fig. 1c; normalized mean bias (NMB) = -44%) and  $PM_{2.5\_CMAQ}$  (Fig. 1d; NMB = -17%) in summer. These concurrent underestimates should be reduced by taking the ratio. We find  $PM_{2.5\_CMAQ}/AOD_{CMAQ}$  is overall consistent with the observed  $PM_{2.5}/AOD$  sampled at co-located AQS-AERONET sites (NMB = 0.9%). AOD distributions retrieved from MODIS ( $AOD_{MAIAC}$ ) agree better with AERONET AOD than  $AOD_{CMAQ}$  (NMB = 5%, Fig. 1f), though we find small low biases at two sites in New York City and at most DRAGON sites over Maryland. Our derived distribution of  $PM_{2.5\_MAIAC}$  is thus closer to  $PM_{2.5}$  observed at AQS sites than  $PM_{2.5\_CMAQ}$  (NMB = 4.7% vs. 44% for  $PM_{2.5\_CMAQ}$ , Fig. 1g). However, the  $PM_{2.5\_MAIAC}$  distribution is wider than observed at AQS: the lowest 5% is 5 vs. 7  $\mu\text{g}/\text{m}^3$  for  $PM_{2.5\_MAIAC}$  vs. AQS  $PM_{2.5}$ , and the highest 5% is 16 vs. 13  $\mu\text{g}/\text{m}^3$ . We find that  $PM_{2.5\_MAIAC}$  is biased high over New York City, coastal regions of Massachusetts, on the borders of upstate New York, and northern Vermont. Evaluation of  $PM_{2.5\_MAIAC}$  in other seasons show larger biases and uncertainties (Fig. S1). In the following sections, we will discuss in detail the sources of uncertainties and biases of satellite-derived  $PM_{2.5}$ . We quantify the uncertainties in terms of bias (systematic) and random uncertainty. The bias uncertainty is linked to the overall accuracy, while the random uncertainty reflects random fluctuations in measurements or the imprecision of the model resulting from imperfect modeling assumptions and simplifications.



### 3.2 Evaluation of satellite observed AOD

AOD<sub>MAIAC</sub> in general agrees well with AERONET observations with spatial  $R = 0.83$ , temporal  $R = 0.85$ ,  $MB = -0.01$ , and  $RMSE = 0.07$ . The performance of AOD<sub>MAIAC</sub> evaluated at Northeast US AERONET sites is consistent with evaluation of Superczynski et al. (2017) over North America ( $R = 0.82$ ,  $MB = -0.008$ ). We find, however, that AOD<sub>MAIAC</sub> in winter (December-5 January-February, DJF) is biased high by 49% ( $MB = +0.02$ ) on average. The wintertime overestimate is likely due to residual snow contamination which is below the detection limit, even though we applied a stringent data quality filter to remove pixels flagged as snow. We find the wintertime overestimate is most evident over northern latitudes (e.g. AERONET sites in Massachusetts, NMB ranges from 80% to 180%), where snow occurs more often. The NMB of AOD<sub>MAIAC</sub> are 15% in MAM, -5% in JJA, and 17% in SON respectively, though the quantile range of the error is large, suggesting that single observations have large random uncertainties (Fig. 2). Taking the  $1\sigma$  standard deviation of the normalized biases as a metric of random uncertainty, we estimate the uncertainties of daily satellite observations to be around 80% in DJF, 60% in MAM and SON, and 50% in JJA. Spatial and/or temporal averaging can reduce random errors of satellite observations, which is evidenced as the smaller spread of errors that for monthly averages at the same spatial resolution, or daily data at coarser (10km) resolution, but it does not reduce the overall MB between AOD<sub>MAIAC</sub> and AOD<sub>AERONET</sub> (Fig. 2). We find that spatially averaging AOD<sub>MAIAC</sub> to 10 km leads to an overall increase of AOD<sub>MAIAC</sub>. Temporal averaging, on the other hand, leads to an overall decrease in AOD<sub>MAIAC</sub> except for DJF, leading to smaller positive MB in SON (7%) and MAM (7%), while larger negative MB in JJA (-8%) and positive MB (67%) in DJF. 10 15 20



### 3.3 Evaluation of modeled $PM_{2.5}/AOD$ relationships

Three factors contribute to the overall uncertainty in the modeled  $PM_{2.5}/AOD$  relationship:  
1)  $PM_{2.5\_CMAQ}$ ; 2)  $AOD_{CMAQ}$ ; 3) the relation between 1) and 2). We evaluate uncertainties of the  
three factors at 13 paired AQS-AERONET sites (within 10 km of each other; about the resolution  
5 of CMAQ). Figure 3 shows the distribution of the biases of modeled daily  $PM_{2.5\_CMAQ}$ ,  $AOD_{CMAQ}$   
and  $PM_{2.5\_CMAQ}/AOD_{CMAQ}$  compared with observations. Generally,  $PM_{2.5\_CMAQ}$  biases vary  
seasonally: from +42% in DJF to -39% in JJA on average. In contrast,  $AOD_{CMAQ}$  biases show  
weaker seasonality. The normalized MBs of  $AOD_{CMAQ}$  are 3% in DJF, -16% in MAM, -7% in JJA  
and -20% in SON. On the daily scale, biases of  $AOD_{CMAQ}$  are weakly correlated with the biases of  
10  $PM_{2.5\_CMAQ}$  ( $R = 0.14$ ), suggesting model biases in AOD do not necessarily reflect biases in  
modeled  $PM_{2.5}$ . This is in contrast with prior analysis at the global annual scale where emission  
biases drive similar biases in AOD and  $PM_{2.5}$  (van Donkelaar et al., 2013). The better accuracy of  
emissions in the Northeast USA than elsewhere in the world allows processes other than emissions  
to be more important for the Northeast USA. We find the seasonal biases in modeled  $PM_{2.5}$  are  
15 retained in the  $PM_{2.5\_CMAQ}/AOD_{CMAQ}$  ratio, which is even larger than the biases of  $PM_{2.5\_CMAQ}$  in  
DJF, MAM and SON. As both  $PM_{2.5\_CMAQ}$  and  $AOD_{CMAQ}$  are biased low in JJA, the modeled  
 $PM_{2.5}/AOD$  bias (-20%) is smaller than that of  $PM_{2.5\_CMAQ}$  (-39%). Biases in  $PM_{2.5\_CMAQ}$  and  
 $AOD_{CMAQ}$  are oppositely signed in fall, leading to largest mean biases of modeled  $PM_{2.5}/AOD$   
(+74%). The spread of the biases of  $PM_{2.5\_CMAQ}/AOD_{CMAQ}$  is larger than that of  $PM_{2.5\_CMAQ}$  and  
20  $AOD_{CMAQ}$ , with the standard deviation ranging from 50% in JJA to 100% in SON.





### 3.4 Relative importance of satellite AOD vs. modeled $PM_{2.5}/AOD$ to uncertainties in satellite-derived $PM_{2.5}$

We have shown that both satellite AOD and modeled  $PM_{2.5}/AOD$  are subject to large uncertainties at the daily time-scale. To directly compare the relative importance of the biases of satellite AOD vs. model  $PM_{2.5}/AOD$  on the satellite-derived  $PM_{2.5}$ , we scale the biases of modeled  $PM_{2.5}/AOD$  with daily  $AOD_{MAIAC}$ , so that the biases are expressed as the unit of  $PM_{2.5}$  ( $\mu\text{g}/\text{m}^3$ ):

$$\Delta PM_{2.5\_AOD} = (AOD_{MAIAC} - AOD_{AERONET}) \times \frac{PM_{2.5\_CMAQ}}{AOD_{CMAQ}} \quad (8)$$

We then scale the of biases of  $AOD_{MAIAC}$  with daily modeled  $PM_{2.5}/AOD$  relationship:

$$\Delta PM_{2.5\_Rel} = \left( \frac{PM_{2.5\_CMAQ}}{AOD_{CMAQ}} - \frac{PM_{2.5\_AQS}}{AOD_{AERONET}} \right) \times AOD_{MAIAC} \quad (9)$$

We can also interpret  $\Delta PM_{2.5\_AOD}$  and  $\Delta PM_{2.5\_Rel}$  as the changes in derived  $PM_{2.5}$  if ‘true’ observed AOD or  $PM_{2.5}/AOD$  instead of  $AOD_{MAIAC}$  or modeled  $PM_{2.5}/AOD$ . As shown in Fig. 4a, mean biases caused by modeled  $PM_{2.5}/AOD$  are  $+9.2 \mu\text{g}/\text{m}^3$  in DJF,  $+2.8 \mu\text{g}/\text{m}^3$  in MAM,  $-3.3 \mu\text{g}/\text{m}^3$  in JJA, and  $+7.7 \mu\text{g}/\text{m}^3$  in SON respectively, which introduces larger biases to the derived  $PM_{2.5}$  than the MAIAC satellite product in all seasons ( $7.6 \mu\text{g}/\text{m}^3$  in DJF,  $+1.3 \mu\text{g}/\text{m}^3$  in MAM,  $-0.7 \mu\text{g}/\text{m}^3$  in JJA, and  $0.9 \mu\text{g}/\text{m}^3$  in SON). Overall, satellite AOD contributes an error (root mean squared  $\Delta PM_{2.5\_AOD}$ ) of  $8.3 \mu\text{g}/\text{m}^3$  to daily satellite  $PM_{2.5\_MAIAC}$  with smallest error in JJA ( $5.1 \mu\text{g}/\text{m}^3$ ) and largest error in DJF ( $13.2 \mu\text{g}/\text{m}^3$ ), while modeled  $PM_{2.5}/AOD$  contributes an error of  $10.8 \mu\text{g}/\text{m}^3$  (root mean squared  $\Delta PM_{2.5\_Rel}$ ) with smallest error in JJA ( $6.5 \mu\text{g}/\text{m}^3$ ) and largest error in SON ( $15.2 \mu\text{g}/\text{m}^3$ ). The spread of the biases is larger for modeled  $PM_{2.5}/AOD$  than that for MAIAC AOD except for DJF. Our findings are consistent with Ford and Heald (2016), who estimate two times larger uncertainties in modeled  $PM_{2.5}/AOD$  relationships than observations using a higher-resolution (nested) version of the GEOS-Chem model and MODIS Dark Target AOD (Collection 6).



At the daily time scale, both  $\Delta\text{PM}_{2.5\_AOD}$  and  $\Delta\text{PM}_{2.5\_Rel}$  show large day-to-day variability: the  $1\sigma$  standard deviation is  $10.5 \mu\text{g}/\text{m}^3$  for daily  $\Delta\text{PM}_{2.5\_AOD}$  and  $8.3 \mu\text{g}/\text{m}^3$  or daily  $\Delta\text{PM}_{2.5\_Rel}$ . Next, we evaluate the dependence of the biases of satellite-derived  $\text{PM}_{2.5}$  (denoted as  $\Delta\text{PM}_{2.5\_MAIAC}$ , evaluated with AQS observed  $\text{PM}_{2.5}$ ) on  $\Delta\text{PM}_{2.5\_Rel}$  versus  $\Delta\text{PM}_{2.5\_AOD}$  by evaluating the Pearson correlation coefficients (R). Overall,  $\Delta\text{PM}_{2.5\_MAIAC}$  is more strongly correlated with  $\Delta\text{PM}_{2.5\_Rel}$  (R = 0.85) than that with  $\Delta\text{PM}_{2.5\_AOD}$  (R = 0.53), indicating the uncertainties of modeled  $\text{PM}_{2.5}/\text{AOD}$  are a more important driving factor to the uncertainties of daily satellite-derived  $\text{PM}_{2.5}$ , which could explain 72% variance ( $R^2$ ) in  $\Delta\text{PM}_{2.5\_MAIAC}$ . In JJA, however,  $\Delta\text{PM}_{2.5\_MAIAC}$  is moderately correlated with both  $\Delta\text{PM}_{2.5\_AOD}$  (R = 0.48) and  $\Delta\text{PM}_{2.5\_Rel}$  (R = 0.49), suggesting uncertainties of modeled  $\text{PM}_{2.5}/\text{AOD}$  and satellite AOD contribute equally to the uncertainties of satellite-derived  $\text{PM}_{2.5}$ . We note that there is no statistically significant correlation between  $\Delta\text{PM}_{2.5\_Rel}$  and  $\Delta\text{PM}_{2.5\_AOD}$ , with R ranging from -0.4 in SON to 0.23 in JJA, which suggests the errors caused by models and that caused by satellite AOD are independent of each other.

### 3.5 Factors leading to uncertainties in modeled $\text{PM}_{2.5}/\text{AOD}$ relationship

Uncertainties in the modeled  $\text{PM}_{2.5}/\text{AOD}$  relationship mainly reflect uncertain aerosol speciation, aerosol vertical profiles, ambient RH, and parameterizations for aerosol optical properties including aerosol density, size distribution, refractive index and hygroscopic growth. Here we quantify the uncertainties from each factor and evaluate their impacts on the derived  $\text{PM}_{2.5}$ .

#### 3.5.1 Aerosol speciation

Aerosol optical properties vary with chemical composition. Model biases in the aerosol composition also affect the overall particle hygroscopicity. For the same  $\text{PM}_{2.5}$  abundance, variations in the aerosol composition may alter the particle optical properties especially hygroscopicity, and consequently the  $\text{PM}_{2.5}/\text{AOD}$  relationship. Fig. 5a compares the modeled



aerosol composition with ground-based observations averaged for each season. High biases in  $PM_{2.5\_CMAQ}$  in winter are largely due to model overestimates of OC by a factor of three, and low biases in summer are due to a combination of underestimated SNA and OC. As a result, CMAQ overestimates the fraction of OC by about 20% in DJF, 15% in MAM, and less than 10% in other  
5 seasons, while underestimates the fraction of SNA by 5% to 20% in all seasons.

To estimate the impacts of model biases in aerosol speciation on  $AOD_{CMAQ}$  and  $PM_{2.5\_MAIAC}$ , we keep the total aerosol mass the same, and redistribute AOD ( $AOD_{CMAQ\_ir}$ ) of each species  $i$  based on observed fraction of each species (i.e. SNA, OC, EC, soil dust; sea salt was excluded due to the limited ground-based measurements and its negligible contribution):

$$10 \quad AOD_{CMAQ\_ir} = \frac{PM_{i\_obs}}{PM_{TOT\_obs}} \times \frac{PM_{TOT\_CMAQ}}{PM_{i\_CMAQ}} \times AOD_{CMAQ\_i} \quad (10)$$

where  $PM_{TOT\_obs}$  and  $PM_{TOT\_CMAQ}$  are the total aerosol mass from observations and CMAQ respectively, which are reconstructed by summing up SNA, OC, EC and soil dust. Next, we estimate the uncertainty due to speciation as the differences in derived  $PM_{2.5\_MAIAC}$  ( $\Delta PM_{2.5\_spe}$ ) using the redistributed  $AOD_{CMAQ\_ir}$  instead of the original  $AOD_{CMAQ}$ , shown in Fig. 5b. As SNA  
15 generally has the largest mass extinction efficiency, a low bias in SNA leads to an overall underestimate of  $AOD_{CMAQ}$ , and therefore an overestimate of  $PM_{2.5\_MAIAC}$ , which is largest in winter (MB = 2.2  $\mu\text{g}/\text{m}^3$ , SD = 2.6  $\mu\text{g}/\text{m}^3$ ) and smallest in summer (MB = 0.7  $\mu\text{g}/\text{m}^3$ , SD = 3.0  $\mu\text{g}/\text{m}^3$ ). The estimated biases due to speciation show similar seasonal cycles as the modeled  $PM_{2.5}/AOD$  biases (Fig. 3c), suggesting that aerosol speciation errors contribute to the seasonality  
20 in modeled  $PM_{2.5}/AOD$  biases. Overall, model-observation discrepancy in speciation causes an error (root mean squared  $\Delta PM_{2.5\_spe}$ ) of 4.0  $\mu\text{g}/\text{m}^3$ . On a daily basis, the correlation (R) between  $\Delta PM_{2.5\_spe}$  and  $\Delta PM_{2.5\_MAIAC}$  is over 0.5 for all seasons except JJA, which means model biases in speciation alone can explain more than 25% variance ( $R^2$ ) in  $\Delta PM_{2.5\_MAIAC}$ . Biases in speciation



in JJA have relatively smaller impacts on the derived  $PM_{2.5}$ , which contribute less than  $1 \mu\text{g}/\text{m}^3$  MB and shows weak correlation with  $\Delta PM_{2.5\_MAIAC}$  ( $R = 0.15$ ).

### 3.5.2 Aerosol vertical profile

A caveat on the results in the Sect. 3.5.1 is that we assume the model errors in speciation  
5 are constant across all vertical layers, as AQS sites only provide observations near the surface. The DISCOVER-AQ aircraft campaign measured vertical variations in aerosol composition, although spatial and temporal coverage is limited. Figure 6a compares the modeled and observed vertical distributions of SNA, OC and BC averaged over the DISCOVER-AQ campaign. We do not discuss sea salt and dust here since they contribute a negligible portion of the total aerosol mass in this  
10 region. Both model and observations show SNA contributes more than half of the total aerosol across all vertical layers (Fig. 6). Aircraft observations show SNA decreases gradually with altitude with a nearly constant vertical gradient, while  $SNA_{CMAQ}$  is well mixed below 1.5 km, and starts to decline at the same rate as  $SNA_{aircraft}$  above 1.5 km (Fig. 6). CMAQ underestimates SNA below 1.5 km, but overestimates SNA at higher altitudes. The positive model bias of SNA at higher  
15 altitudes may be due to excessive vertical transport, or overestimation of RH (Sect. 3.4.3) and consequently overestimation of  $SO_2$  oxidation rate. OC, on the other hand, is biased low at all altitudes, which is likely due to inaccurate treatments in the production of secondary organic aerosol (Zhang et al., 2009). The newer version of CMAQv5.1 shows higher SOA concentration in summer with the introduction of new SOA species (Appel et al., 2017). BC is generally low  
20 during the campaign (typically lower than  $0.3 \mu\text{g}/\text{m}^3$ ).  $BC_{CMAQ}$  generally agrees well with  $BC_{aircraft}$ , though  $BC_{CMAQ}$  tends to overestimate BC between 1 km and 3 km. Figure 6b compares CMAQ modeled and observed total aerosol mass ( $SNA + OC + BC$ ) averaged during the campaign.



CMAQ modeled aerosol mass is on average biased low below 2 km, and biased high at higher altitudes (Fig. 6b).

Next, we evaluate how the vertical distribution of aerosols relates to extinction. Figure 6c compares the modeled and observed average vertical extinction profiles. We find, consistent with  
5 the biases in mass, a low bias in the modeled extinction profile below 2 km, and high bias above (Fig. 6c). The biases in extinction and the biases in mass have the same signs for more than 80% of data pairs, are strongly correlated ( $R = 0.85$ ). This suggests that the aerosol vertical profile of extinction is mainly indicative of mass distribution. However, column AOD measures the vertical integral of light extinction by aerosols, which means the modeled AOD biases would be  
10 proportional to modeled surface  $PM_{2.5}$  biases only if the biases in extinction are constant across all vertical layers. Since the biases of extinction change sign at higher altitude, the AOD biases reflect the competing effects of negative biases near the surface and positive biases at high altitudes, which lead to an overall negative bias of  $PM_{2.5}/AOD$  relationship, consistent with the negative NMB of  $PM_{2.5}/AOD$  in July shown in Fig. 3c.

15 To explore the causes of the model-observation discrepancy in extinction and the resulting impacts on the satellite-derived surface  $PM_{2.5}$ , we calculate the vertical extinction profile in CMAQ by replacing the modeled aerosol mass distribution (SNA, OC, BC), or total mass extinction efficiency (MEE, total aerosol mass/extinction), or RH respectively with those of the aircraft observations, as shown in Fig. 7a. Replacing the modeled aerosol mass with observations,  
20 we find a decrease in extinction at high altitudes (above 2.5 km) and increase at low altitudes (below 2.5 km), but replacing the aerosol mass alone does not explain all of the model-observation differences. At high altitudes, only replacing the modeled total mass extinction efficiency without changing the mass captures the observed extinction. We attribute the model overestimate of



extinction to model overestimation of extinction efficiency at high altitudes. A major contributor to the model overestimate of total MEE is its excessive RH at high altitudes, which leads to an overestimate of the hygroscopic growth. Replacing RH with observations largely corrects the high biases aloft, but does not correct the low biases below 2 km remain (Fig. 7a). At lower altitudes, the model low biases are due to model underestimates of both aerosol mass and total MEE. Model underestimates of MEE are likely due to: 1) model uncertainties of the optical properties; 2) other aerosols or gases (e.g. NO<sub>2</sub>, O<sub>3</sub>) or liquid clouds that can scatter or absorb light.

Figure 7b shows the biases of PM<sub>2.5\_MAIAC</sub> due to model uncertainties in vertical profiles of aerosol mass or MEE or RH, estimated by calculating the changes in PM<sub>2.5</sub> when we replace the model vertical profiles with observations. Since the altitude of the aircraft observation ranges from 0.3 to 3.4 km, we use modeled values for the layers below 0.3 km and above 3.4 km while attempting to minimize the discontinuity at both boundaries through vertical interpolation. As SNA and OC contribute most to extinction, we also evaluate the biases of vertical profiles of SNA and OC separately. We find that replacing modeled aerosol mass with observed mass leads to small positive biases in PM<sub>2.5\_MAIAC</sub> (MB = 0.05 μg/m<sup>3</sup>, SD = 4.3 μg/m<sup>3</sup>), due to the combined effects of negative biases from SNA (MB = -2.5 μg/m<sup>3</sup>, SD = 4.7 μg/m<sup>3</sup>) and positive biases from OC (MB = +1.9 μg/m<sup>3</sup>, SD = 4.3 μg/m<sup>3</sup>).

We further separate the model-observation discrepancy in the vertical profiles as differences in total column mass versus in vertical profile shape by 1) keeping the modeled vertical distribution but adjusting the mass of each species uniformly so that the total column mass is equal to observation; 2) keeping the total column mass the same as in the model but redistributing the aerosol based on the observed vertical profiles. We find that redistributing the aerosol vertical profile leads to a positive mean bias in PM<sub>2.5\_MAIAC</sub> (MB = 1.1 μg/m<sup>3</sup>, SD = 4.9 μg/m<sup>3</sup>), while the



model-observation discrepancy in column mass leads to a negative mean bias ( $MB = -0.6 \mu\text{g}/\text{m}^3$ ,  $SD = 3.6 \mu\text{g}/\text{m}^3$ ) (Fig. 7b). The positive biases in the profile shape are mainly attributed to model biases of the vertical profile of SNA ( $MB = 1.2 \mu\text{g}/\text{m}^3$ ,  $SD = 5.0 \mu\text{g}/\text{m}^3$ ), which shows a larger fraction of SNA at higher altitude where aerosol is less effective at scattering light due to lower  
5 RH. The negative MB of column mass reflects a combination of negative biases of SNA ( $MB = -4.1 \mu\text{g}/\text{m}^3$ ,  $SD = 5.6 \mu\text{g}/\text{m}^3$ ) due to model overestimates of SNA column mass, and positive bias of OC ( $MB = 6.7 \mu\text{g}/\text{m}^3$ ,  $SD = 4.4 \mu\text{g}/\text{m}^3$ ) due to model underestimate of column mass of OC. Model biases in mass extinction efficiency lead to a small positive MB of  $0.6 \mu\text{g}/\text{m}^3$ .

Using the observed  $PM_{2.5}/AOD$  acquired from paired AQS-AERONET sites, we estimate  
10 that model biases in modeled  $PM_{2.5}/AOD$  lead to a negative MB of  $-0.9 \mu\text{g}/\text{m}^3$  with large day-to-day variability ( $SD = 9.8 \mu\text{g}/\text{m}^3$ ) during the DISCOVER-AQ campaign, reflecting the model biases from different sources as discussed above. Next, we evaluate which factor drives the daily variability in the modeled  $PM_{2.5}/AOD$  biases the most by evaluating R value between the estimated biases in modeled  $PM_{2.5}/AOD$  vs. that attributed to individual factors. We find model bias in  
15 aerosol mass is the most deterministic factor for the biases in modeled  $PM_{2.5}/AOD$  ( $R = 0.82$ , Fig. 7c). Model biases in aerosol mass can be due to either biases in column mass or vertical profile shape. We find model biases in modeled  $PM_{2.5}/AOD$  are more dependent on the biases in aerosol column mass ( $R = 0.79$ ), instead of vertical profile shape. Model biases in mass extinction efficiency show moderate correlation with model biases of  $PM_{2.5}/AOD$  ( $R = 0.56$ ). While model  
20 uncertainties in RH lead to an overall negative bias ( $MB = -1.7 \mu\text{g}/\text{m}^3$ ,  $SD = 7.4 \mu\text{g}/\text{m}^3$ ) to  $PM_{2.5\_MAIAC}$ , they are negatively correlated with model biases of  $PM_{2.5}/AOD$  ( $R = -0.25$ ).



### 3.5.3 RH

Figure 7 suggests model biases in RH contribute a negative bias to the derived  $PM_{2.5\_MAIAC}$  during the DISCOVER-AQ aircraft campaign. Here we evaluate the impacts of modeled RH ( $RH_{CMAQ}$ ) biases on derived  $PM_{2.5}$  throughout the year using six atmospheric soundings over the Northeast USA. We only assess the impacts of RH on the optical properties (i.e. hygroscopic growth) of aerosols. Comparing  $RH_{CMAQ}$  with observed RH ( $RH_{obs}$ ),  $RH_{CMAQ}$  is overall biased high with the largest biases in winter. To evaluate the resulting impacts on  $AOD_{CMAQ}$ , we recalculate the extinction using observed ambient RH from the soundings instead of  $RH_{CMAQ}$  in Eq. (4), as shown in Fig. 8. Replacing  $RH_{CMAQ}$  with  $RH_{obs}$  decreases extinction by ~50% on average from the surface to 5km in both JJA and DJF (black lines in Fig. 8a and b). As AOD is the vertical integral of extinction, the total area between  $EXT_{sonde}$  and  $EXT_{CMAQ}$  (gray shading in Fig. 8 a and b) indicates the differences in AOD due to differences in RH. The differences in RH below 3km in DJF, MAM and SON contribute more than 80% to the total differences in AOD. In JJA, the contribution from higher versus lower altitudes is similar, despite model biases of RH are small below 2 km.

We evaluate how the model-observation discrepancy in RH affects the derived  $PM_{2.5}$  by calculating the changes in  $PM_{2.5\_MAIAC}$  ( $\Delta PM_{2.5\_RH}$ ) if  $EXT_{sonde}$  is used instead of  $EXT_{CMAQ}$ . As expected, model errors in RH lead to a negative bias in derived  $PM_{2.5\_MAIAC}$  of  $2 \mu g/m^3$  on average (Fig. 8c). The negative biases in  $PM_{2.5\_MAIAC}$  due to RH are largest in spring ( $-3.5 \mu g/m^3$ ), and smallest in summer ( $-1.6 \mu g/m^3$ ). While we find a large spread of  $\Delta PM_{2.5\_RH}$  that extends from -10 to  $5 \mu g/m^3$  (SD =  $4.5 \mu g/m^3$ , RMSE =  $3 \mu g/m^3$ ), there is no significant correlation between  $\Delta PM_{2.5\_RH}$  and  $\Delta PM_{2.5\_MAIAC}$  ( $R = 0.18$ , evaluated at nearby sites within 10 km), suggesting the





model uncertainty in RH is not a main contributor to the random uncertainties in satellite-derived PM<sub>2.5</sub>.

### 3.5.4 Uncertainties in the parameterization of aerosol optical properties

In previous sections, we demonstrated that the satellite-derived PM<sub>2.5</sub> depends on the accuracy of the model simulation. Even with a perfect simulation, satellite-derived PM<sub>2.5</sub> will be sensitive to the parameterization of aerosol optical properties, which would affect the mass-extinction efficiency. We evaluate the uncertainties associated with the parameterization of aerosol optical properties by varying each parameter (Table 1), and calculate the corresponding changes in the derived PM<sub>2.5\_MAIAC</sub>. Figure 9 shows the range of uncertainty in annual average PM<sub>2.5\_MAIAC</sub> due to uncertain aerosol size distributions, hygroscopicity, refractive index and aerosol species density.

The size of a particle is a defining characteristic of aerosol light extinction (Mishchenko et al., 1999). To evaluate model sensitivities to the uncertainties in size distribution, we vary the  $r_0$  of SNA from 0.05 to 0.15 with a 0.02 increase each time, to cover the range of values reported in the literature. For OC, we calculate AOD<sub>CMAQ</sub> with  $r_0 = 0.02, 0.06, 0.09$  and  $0.12 \mu\text{m}$ , all values used in previous studies (Hess et al., 1998; Chin et al., 2002; Highwood, 2009; Drury et al., 2010). Annual average PM<sub>2.5\_MAIAC</sub> could vary by up to  $5 \mu\text{g}/\text{m}^3$  (32%) with the choice of modal radius of either  $r_{\text{SNA}}$  or  $r_{\text{OC}}$ , which is the largest source of uncertainty among the four parameters (Fig. 9). We find that AOD<sub>CMAQ</sub> reaches a maximum with  $r_{\text{SNA}} = 0.07 \mu\text{m}$  ( $r_{\text{eff}} = 0.12 \mu\text{m}$ ), and minimum with  $r_{\text{SNA}} = 0.05$  ( $r_{\text{eff}} = 0.15 \mu\text{m}$ ), while PM<sub>2.5\_MAIAC</sub> reaches a maximum with  $r_{\text{SNA}} = 0.05$  ( $r_{\text{eff}} = 0.09 \mu\text{m}$ ), and minimum with  $r_{\text{SNA}} = 0.11$  ( $r_{\text{eff}} = 0.19 \mu\text{m}$ ), suggesting the impacts of size distribution are nonlinear and non-uniform (Fig. S3). Mie scattering of a particle tends to be most effective when the particle's diameter is near the wavelength of interest ( $0.55 \mu\text{m}$ ). As hygroscopic



particle growth also affects the size distribution, depending on ambient RH and the hygroscopic growth factor, reducing (or increasing) the dry effective radius could either lead the bulk aerosol size closer to or further from  $0.55 \mu\text{m}$ , and thus an increase or decrease in the extinction. For OC, as the effective radius and the hygroscopic growth factor are smaller than that of SNA, increasing the modal radius leads to more effective scattering, thus larger  $\text{AOD}_{\text{CMAQ}}$  and smaller  $\text{PM}_{2.5\_MAIAC}$ . Relative to the default  $r_{\text{OC}} = 0.09 \mu\text{m}$  as assumed in Drury et al. (2010), using the  $r_{\text{OC}}$  ( $0.02 \mu\text{m}$ ) recommended by Chin et al. (2002a) increases  $\text{PM}_{2.5\_MAIAC}$  by  $5 \mu\text{g}/\text{m}^3$  (32%) on average, which would worsen the positive biases of  $\text{PM}_{2.5\_MAIAC}$ . Increasing  $r_{\text{OC}}$  to  $0.12 \mu\text{m}$  as recommended by Highwood et al. (2009) has little effect, decreasing  $\text{PM}_{2.5\_MAIAC}$  by 2% on average.

The uncertainty of hygroscopicity lies in two aspects: the variations of the function shape and the uncertainties in the parameters. Figure S2 compares the function shape of  $\kappa$  function with the hygroscopic growth factors used by the IMPROVE network (Hand and Malm, 2006) and the default algorithm used for online calculation of AOD in CMAQ and that proposed by Chin et al. (2002) (Table 1). Using the DISCOVER-AQ aircraft data to evaluate the parameterization of hygroscopic growth, we find that the  $\kappa$  parameter best characterizes the observed hygroscopic growth factor (Fig. S2c). Latimer and Martin (2018) similarly found that implementing a  $\kappa$  formulation instead of hygroscopic growth based on OPAC improved the GEOS-Chem representation of mass scattering efficiency. Thus, we choose the  $\kappa$  parameter to represent the hygroscopic growth factor, and the uncertainty estimate here only reflects the uncertainties with parameter  $\kappa$ . In practice changes in aerosol composition could have even larger effects on hygroscopicity than uncertainties in  $\kappa$  as discussed in Sect. 3.5.1.

To test the uncertainties of  $\kappa$  parameter, we compute  $\text{AOD}_{\text{CMAQ}}$  using the low (0.33) and high end of  $\kappa$  (0.72) for SNA as suggested by Koehler et al. (2006). As the hygroscopic properties



of inorganic salts are relatively well-known, the range of uncertainty for  $f(\text{RH})$  of SNA is 30% at most (Fig. S2b). OC, on the other hand, is composed of thousands of species with distinct hygroscopicities. Assuming  $\kappa_{\text{OC}}$  ranges from 0 (non-hygroscopic) to 0.2 (Jimenez et al., 2009; Duplissy et al., 2011), the range of  $f(\text{RH})$  of OC can be as large as a factor of 2 at high  $\text{RH} > 96\%$  (Fig. S2a). Despite the larger uncertainty of  $\kappa_{\text{OC}}$ , we find the overall impacts of the uncertainties of  $\kappa_{\text{OC}}$  on the derived  $\text{PM}_{2.5}$  ( $0.3 \mu\text{g}/\text{m}^3$ , 2% of annual average  $\text{PM}_{2.5\_MAIAC}$ ) are smaller than that of  $\kappa_{\text{SNA}}$  ( $1.6 \mu\text{g}/\text{m}^3$ , 11% of annual average  $\text{PM}_{2.5\_MAIAC}$ ). The small impacts of  $\kappa_{\text{OC}}$  reflect the relatively small portion and the less hygroscopic nature of OC. For single observations, varying  $\kappa_{\text{SNA}}$  leads to a maximum increase in  $\text{PM}_{2.5\_MAIAC}$  by 20% and a maximum decrease by 28%. Varying  $\kappa_{\text{OC}}$  increases  $\text{PM}_{2.5\_MAIAC}$  by 10% or decrease  $\text{PM}_{2.5\_MAIAC}$  by 18% at most. The overall impact of the uncertainties of  $\kappa_{\text{SNA}}$  ranks the second among the four parameters for SNA, while  $\kappa_{\text{OC}}$  has the smallest impacts on the derived  $\text{PM}_{2.5}$  (Fig. 9).

The refractive index ( $m$ ) determines the Mie extinction efficiency, which is subject to uncertainties mostly due to the lack of measurements (Kanakidou et al., 2005).  $m_{\text{SNA}}$  in OPAC (default value) is slightly different from that recommended in Chin et al. (2002) and Highwood (2009). Moise et al. (2015) suggest  $m_{\text{OC}}$  varies by species, with its real part ranging from 1.37 to 1.65. We calculated additional  $\text{AOD}_{\text{CMAQ}}$  by varying the real part of  $m_{\text{SNA}}$  and  $m_{\text{OC}}$  using the lowest and highest values reported in the literature. We find the annual average  $\text{PM}_{2.5\_MAIAC}$  decreased by  $0.8 \mu\text{g}/\text{m}^3$  (6%) using the high end of  $m_{\text{R\_SNA}}$ , while increased by  $1.3 \mu\text{g}/\text{m}^3$  (9%) on average using the low end. Though  $M_{\text{R\_OC}}$  has a wider range of uncertainty, its impacts on  $\text{PM}_{2.5\_MAIAC}$  (-4% to +6%) are smaller than that of  $M_{\text{R\_SNA}}$ . While the overall impacts on  $\text{PM}_{2.5\_MAIAC}$  due to uncertainties of  $M_{\text{R\_SNA}}$  are generally within 10% for single observations,  $\text{PM}_{2.5\_MAIAC}$  can change by more than 20% under SNA dominated and high RH environments. The overall uncertainty due



to  $M_{R\_OC}$  is generally within 5% for single observations, with a few cases (<10% of the total data) where the relative change in  $PM_{2.5\_MAIAC}$  can exceed 10%.

As aerosol density ( $\rho$ ) is assumed to be constant for each species, varying  $\rho$  has the same effect on the extinction of given species. We vary the aerosol density of SNA from 1.65 to 1.83 g/cm<sup>3</sup> based on the uncertainty estimate from a laboratory study of Sarangi et al. (2016), which translates to an uncertainty of -3% to 7% for  $AOD_{SNA}$ , and the aerosol density of OC from 1.2 to 1.78 g/cm<sup>3</sup> following Park et al. (2006), which translates to an uncertainty in  $AOD_{OC}$  ranging from -8% to 37%. We find aerosol species density, in general, contributes the smallest uncertainty to the satellite-derived  $PM_{2.5}$ . Varying  $\rho_{oc}$  leads to annual average  $PM_{2.5\_MAIAC}$  increased by 0.9  $\mu\text{g}/\text{m}^3$  (6%) and decreased by 0.6  $\mu\text{g}/\text{m}^3$  (3%) at most. As the aerosol density of inorganic salt is less uncertain, varying  $\rho_{sulf}$  leads to negligible changes in annual average  $PM_{2.5\_MAIAC}$  at both high (0.7  $\mu\text{g}/\text{m}^3$ , 5%) and low ends (-0.5  $\mu\text{g}/\text{m}^3$ , -2%).

#### 4 Conclusions

We derive surface  $PM_{2.5}$  distributions from satellite observations of AOD (MAIAC products) at 1 km resolution for 2011 over the Northeast USA using a geophysical approach that simulates the relationship between surface  $PM_{2.5}$  and AOD with a regional air quality model (CMAQ) and offline AOD calculation package (FlexAOD). We find the fine spatial resolution of MAIAC AOD reveals more spatial details such as hot spots over populated urban areas or along major roadways. While the geophysical approach has shown promising values for mapping the  $PM_{2.5}$  exposure at seasonal to annual scale (van Donkelaar et al., 2010; 2016), we show that estimating  $PM_{2.5}$  from satellite AOD at the daily scale is not only subject to large measurement uncertainties of satellite observations, but more importantly, to uncertainty in daily variations of the relationship between surface  $PM_{2.5}$  and column AOD. We take advantage of multi-platform *in*



*situ* observations available over the Northeast USA to quantify different sources of uncertainties in the satellite-derived  $PM_{2.5}$ , especially at the daily scale. We use observed AOD from the AERONET sun photometers to quantify uncertainties in satellite and modeled AOD; co-located AQS  $PM_{2.5}$  and AERONET sites to evaluate modeled  $PM_{2.5}$ /AOD relationships; IMPROVE and  
5 CSN aerosol speciation data to evaluate model uncertainties of aerosol composition; atmospheric soundings to evaluate modeled RH, as well as their impacts on  $PM_{2.5}$  derivation. To assess the uncertainties associated with aerosol vertical profile, we use the extensive concurrent measurements of extinction and aerosol composition available from the NASA DISCOVER-AQ 2011 campaign over Baltimore-Washington, D.C. Finally, we estimate intrinsic uncertainties  
10 associated with the model parameterization of optical properties, by testing sensitivities of satellite-derived  $PM_{2.5}$  to variations in each parameter separately using FlexAOD.

As the relationship between surface  $PM_{2.5}$  and column AOD is non-linear and spatiotemporally heterogeneous, satellite AOD alone is unable to fully resolve the spatial and temporal variability of ground-level  $PM_{2.5}$ . At the seasonal scale, we find large-scale spatial  
15 variability of satellite-derived  $PM_{2.5}$  is more correlated with the spatial variability in modeled  $PM_{2.5}$ /AOD than observed  $AOD_{MAIAC}$ . At the daily scale in the Northeast USA, modeled  $PM_{2.5}$ /AOD introduce larger mean biases to satellite-derived  $PM_{2.5}$  than satellite retrievals, and uncertainties in modeled  $PM_{2.5}$ /AOD explain more than 70% variance in the uncertainties of satellite-derived  $PM_{2.5}$ , suggesting that the precision of daily satellite-derived  $PM_{2.5}$  depends on  
20 the capability of model to simulate the day-to-day variability of the relationship between  $PM_{2.5}$  and AOD.

Uncertainties in modeled  $PM_{2.5}$ /AOD relationships can be attributed to several factors, including uncertain model aerosol speciation, vertical profiles, RH, as well as the parameterization



of aerosol optical properties. We find that seasonally varying biases in modeled  $PM_{2.5}/AOD$  reflect biases in aerosol speciation, particularly OC, which is overestimated in the cold season, and underestimated by CMAQ in the warm season. Biases in aerosol composition in turn affect aerosol hygroscopicity. The CMAQ model generally overestimates RH, especially at high altitudes ( $> 2$  km), which contributes to an overall negative bias to satellite-derived  $PM_{2.5}$ . Using concurrent measurements of vertical profiles of aerosol extinction and composition available from the DISCOVER-AQ 2011 aircraft campaign, we show that the aerosol extinction is indicative of mass distributions, but the biases of modeled extinction vary with altitude, meaning that the model biases in vertically integrated column AOD do not necessarily reflect model biases in surface  $PM_{2.5}$ . We attribute uncertainties in modeled vertical profiles to various factors including column mass, profile shape, mass-extinction efficiency and RH. We find that model uncertainties of column mass and the mass-extinction efficiency drive the variability in modeled  $PM_{2.5}/AOD$  uncertainty, while RH and aerosol vertical profile shape contribute some systematic bias.

Even with a model that perfectly simulates the distribution of aerosols, calculating AOD is subject to additional uncertainties in aerosol size distributions, hygroscopic growth factors refractive indices and aerosol density. Our uncertainty analysis involving a series of sensitivity tests in FlexAOD indicates that for SNA, the uncertainties in size distributions contribute most to uncertainty in the derived  $PM_{2.5}$  (32%), followed by the hygroscopicity parameter  $\kappa$  (11%), refractive index (9%), and aerosol density (5%). For OC, size distribution is also the largest source of uncertainty in the derived  $PM_{2.5}$  (32%). Despite the large uncertainty of the hygroscopicity of OC, its impact on the satellite-derived  $PM_{2.5}$  is negligible (2%), even smaller than uncertainties associated with the refractive index and aerosol density (6% each).

Based on this uncertainty analysis, we identify opportunities and directions to develop the



applications of satellite-derived  $PM_{2.5}$  using the geophysical approach, especially at finer spatial and temporal scales. Van Donkelaar et al. (2016) found that calibration with ground-based  $PM_{2.5}$  measurements improves the performance of satellite-based  $PM_{2.5}$  at the annual scale, although such calibration is more challenging at short time scales (van Donkelaar et al., 2012). As the

5 uncertainties of satellite-derived  $PM_{2.5}$  are due to a combination of multiple factors, calibration targeting specific sources of uncertainty would help further refine the geophysical approach. Additional collocated measurements of both  $PM_{2.5}$  and AOD would be valuable to further evaluate the relationship between surface  $PM_{2.5}$  and satellite AOD (Snider et al. 2015). Routine measurements of aerosol vertical profiles would facilitate uncertainty attribution and likely lead to

10 improved models and thereby reduce the overall uncertainty in satellite-derived  $PM_{2.5}$ . Quantifying source-specific uncertainties would not only facilitate future model improvement, but more importantly, benefit applications of the satellite-derived  $PM_{2.5}$  products to health studies.



**Author contribution:** XJ, AF, AD, and RM designed the experiments. GC developed the FlexAOD code for CMAQ. AL provided MAIAC AOD data. KC and MK conducted the CMAQ simulation. XJ carried out the data analysis and prepared the manuscript with contributions from all co-authors.

5 **Acknowledgement:** Support for this study was provided by New York State Energy Research and Development Authority (Grant number: 91268) and NASA Health and Air Quality Applied Sciences Team (HAQAST, Grant NNX16AQ20G). The authors thank Melanie Follette-Cook of NASA GSFC and Morgan State University for her help in obtaining the DISCOVER-AQ aircraft data. We acknowledge useful discussions with Yang Liu from Emory University and Dan  
10 Westervelt from Lamont-Doherty Earth Observatory of Columbia University. Although this manuscript was reviewed internally, it does not necessarily reflect the views or policies of the New York State Department of Environmental Conservation.





## References

- Adams, P. J.: Predicting global aerosol size distributions in general circulation models, *J. Geophys. Res.*, 107(D19), 13,791–AAC 4–23, doi:10.1029/2001JD001010, 2002.
- Appel, K. W., Pouliot, G. A., Simon, H., Sarwar, G., Pye, H. O. T., Napelenok, S. L., Akhtar, F.  
5 and Roselle, S. J.: Evaluation of dust and trace metal estimates from the Community Multiscale Air Quality (CMAQ) model version 5.0, *Geosci. Model Dev.*, 6(4), 883–899, doi:10.5194/gmd-6-883-2013, 2013.
- Appel, K. W., Napelenok, S. L., Foley, K. M., Pye, H. O. T., Hogrefe, C., Luecken, D. J., Bash, J. O., Roselle, S. J., Pleim, J. E., Foroutan, H., Hutzell, W. T., Pouliot, G. A., Sarwar, G.,  
10 Fahey, K. M., Gantt, B., Gilliam, R. C., Heath, N. K., Kang, D., Mathur, R., Schwede, D. B., Spero, T. L., Wong, D. C. and Young, J. O.: Description and evaluation of the Community Multiscale Air Quality (CMAQ) modeling system version 5.1, *Geosci. Model Dev.*, 10(4), 1703–1732, doi:10.5194/gmd-10-1703-2017, 2017.
- Bey, I., Jacob, D. J., Yantosca, R. M., Logan, J. A., Field, B. D., Fiore, A. M., Li, Q. B., Liu, H.,  
15 Mickley, L. J. and Schultz, M. G.: Global modeling of tropospheric chemistry with assimilated meteorology: Model description and evaluation, *J. Geophys. Res. Atmos.*, 106(D19), 23073–23095, doi:10.1029/2001JD000807, 2001.
- Brock, C. A. et al., Aerosol optical properties in the southeastern United States in summer &ndash; Part 1: Hygroscopic growth, *Atmos. Chem. Phys.*, 16(8), 4987–5007, doi:10.5194/acp-16-  
20 4987-2016, 2016
- Chin, M., Ginoux, P., Kinne, S., Torres, O., Holben, B. N., Duncan, B. N., Martin, R. V., Logan, J. A., Higurashi, A. and Nakajima, T.: Tropospheric aerosol optical thickness from the GOCART model and comparisons with satellite and Sun photometer measurements, *Journal of the Atmospheric Sciences*, 59(3), 461–483, doi:10.1175/1520-  
25 0469(2002)059<0461:TAOTFT>2.0.CO;2, 2002.
- Cohen, A. J., Brauer, M., Burnett, R., Anderson, H. R., Frostad, J., Estep, K., Balakrishnan, K., Brunekreef, B., Dandona, L., Dandona, R., Feigin, V., Freedman, G., Hubbell, B., Jobling, A., Kan, H., Knibbs, L., Liu, Y., Martin, R., Morawska, L., Pope, C. A., III, Shin, H., Straif, K., Shaddick, G., Thomas, M., Van Dingenen, R., van Donkelaar, A., Vos, T., Murray, C. J. L. and Forouzanfar, M. H.: Estimates and 25-year trends of the global burden of disease attributable to ambient air pollution: an analysis of data from the Global Burden of Diseases



- Study 2015, *The Lancet*, 389(10082), 1907–1918, doi:10.1016/S0140-6736(17)30505-6, 2017.
- Crouse, D. L. et al., Risk of Nonaccidental and Cardiovascular Mortality in Relation to Long-term Exposure to Low Concentrations of Fine Particulate Matter: A Canadian National-Level Cohort Study, *Environmental Health Perspectives*, 120(5), 708–714, doi:10.1289/ehp.1104049, 2012.
- Crumeyrolle, S., Chen, G., Ziemba, L., Beyersdorf, A., Thornhill, L., Winstead, E., Moore, R. H., Shook, M. A., Hudgins, C. and Anderson, B. E.: Factors that influence surface PM<sub>2.5</sub> values inferred from satellite observations: perspective gained for the US Baltimore–Washington metropolitan area during DISCOVER-AQ, *Atmos. Chem. Phys.*, 14(4), 2139–2153, doi:10.5194/acp-14-2139-2014, 2014.
- Curci, G.: FlexAOD: A Chemistry-transport Model Post-processing Tool for A Flexible Calculation of Aerosol Optical Properties, pp. 1–4, L'Aquila, Italy. 2012.
- Curci, G., Hogrefe, C., Bianconi, R., Im, U., Balzarini, A., Baró, R., Brunner, D., Forkel, R., Giordano, L., Hirtl, M., Honzak, L., Jiménez-Guerrero, P., Knote, C., Langer, M., Makar, P. A., Pirovano, G., Pérez, J. L., José, R. S., Syrakov, D., Tuccella, P., Werhahn, J., Wolke, R., Žabkar, R., Zhang, J. and Galmarini, S.: Uncertainties of simulated aerosol optical properties induced by assumptions on aerosol physical and chemical properties: An AQMEII-2 perspective, *Atmospheric Environment*, 115(c), 541–552, doi:10.1016/j.atmosenv.2014.09.009, 2015.
- de Hoogh, K., Gulliver, J., Donkelaar, A. V., Martin, R. V., Marshall, J. D., Bechle, M. J., Cesaroni, G., Pradas, M. C., Dedele, A., Eeftens, M., Forsberg, B., Galassi, C., Heinrich, J., Hoffmann, B., Jacquemin, B., Katsouyanni, K., Korek, M., Künzli, N., Lindley, S. J., Lepeule, J., Meleux, F., de Nazelle, A., Nieuwenhuijsen, M., Nystad, W., Raaschou-Nielsen, O., Peters, A., Peuch, V.-H., Rouil, L., Udvardy, O., Slama, R., Stempfelet, M., Stephanou, E. G., Tsai, M. Y., Yli-Tuomi, T., Weinmayr, G., Brunekreef, B., Vienneau, D. and Hoek, G.: Development of West-European PM<sub>2.5</sub> and NO<sub>2</sub> land use regression models incorporating satellite-derived and chemical transport modelling data, *Environmental Research*, 151, 1–10, doi:10.1016/j.envres.2016.07.005, 2016.



- Di, Q., Kloog, I., Koutrakis, P., Lyapustin, A., Wang, Y. and Schwartz, J.: Assessing PM<sub>2.5</sub> Exposures with High Spatiotemporal Resolution across the Continental United States, *Environ. Sci. Technol.*, 50(9), 4712–4721, doi:10.1021/acs.est.5b06121, 2016.
- Dockery, D. W., C. A. Pope, X. Xu, J. D. Spengler, J. H. Ware, M. E. Fay, B. G. Ferris Jr., and F. E. Speizer, An Association between Air Pollution and Mortality in Six U.S. Cities, *N Engl J Med*, 329(24), 1753–1759, doi:10.1056/NEJM199312093292401, 1993.
- Dominici, F., Peng, R. D., Bell, M. L., Pham, L., McDermott, A., Zeger, S. L. and Samet, J. M.: Fine Particulate Air Pollution and Hospital Admission for Cardiovascular and Respiratory Diseases, *JAMA*, 295(10), 1127–1134, doi:10.1001/jama.295.10.1127, 2006.
- Drury, E., Jacob, D. J., Spurr, R. J. D., Wang, J., Shinzuka, Y., Anderson, B. E., Clarke, A. D., Dibb, J., McNaughton, C. and Weber, R.: Synthesis of satellite (MODIS), aircraft (ICARTT), and surface (IMPROVE, EPA-AQS, AERONET) aerosol observations over eastern North America to improve MODIS aerosol retrievals and constrain surface aerosol concentrations and sources, *Journal of Geophysical Research: Atmospheres* (1984–2012), 115(D14), D14204, doi:10.1029/2009JD012629, 2010.
- Duplissy, J., DeCarlo, P. F., Dommen, J., Alfarra, M. R., Metzger, A., Barmpadimos, I., Prevot, A. S. H., Weingartner, E., Tritscher, T., Gysel, M., Aiken, A. C., Jimenez, J. L., Canagaratna, M. R., Worsnop, D. R., Collins, D. R., Tomlinson, J. and Baltensperger, U.: Relating hygroscopicity and composition of organic aerosol particulate matter, *Atmos. Chem. Phys.*, 11(3), 1155–1165, doi:10.5194/acp-11-1155-2011, 2011.
- Durre, I., and X. Yin, Enhanced Radiosonde Data for Studies of Vertical Structure, *Bull. Amer. Meteor. Soc.*, 89(9), 1257–1262, 2008. Retrieved from <http://www.jstor.org/stable/26220887>
- Ford, B. and Heald, C. L.: Exploring the uncertainty associated with satellite-based estimates of premature mortality due to exposure to fine particulate matter, *Atmos. Chem. Phys.*, 16(5), 3499–3523, doi:10.5194/acp-16-3499-2016, 2016.
- Green, M., Kondragunta, S., Ciren, P. and Xu, C.: Comparison of GOES and MODIS Aerosol Optical Depth (AOD) to Aerosol Robotic Network (AERONET) AOD and IMPROVE PM<sub>2.5</sub> Mass at Bondville, Illinois, *Journal of the Air & Waste Management Association*, 59(9), 1082–1091, doi:10.3155/1047-3289.59.9.1082, 2012.



- Griffin, D., Naumova, E., McEntee, J., Castronovo, D., Durant, J., Lyles, M., Faruque, F. and Lary, D.: Air quality and human health, in Environmental Tracking for Public Health Surveillance, pp. 129–185, CRC Press. 2012.
- Gupta, P. and Christopher, S. A.: Particulate matter air quality assessment using integrated surface,  
5 satellite, and meteorological products: Multiple regression approach, *J. Geophys. Res.*, 114(D14), 1249–13, doi:10.1029/2008JD011496, 2009.
- Hand, J. and Malm, W. C. Review of the IMPROVE equation for estimating ambient light extinction coefficients, Colorado State University, Fort Collins, 2006.
- Hess, M., Koepke, P. and Schult, I.: Optical Properties of Aerosols and Clouds: The Software  
10 Package OPAC, *Bull. Amer. Meteor. Soc.*, 79(5), 831–844, doi:10.1175/1520-0477(1998)079<0831:OPOAAC>2.0.CO;2, 1998.
- Highwood, E.J., 5 August 2009. Suggested Refractive Indices and Aerosol Size Parameters for Use in Radiative Effect Calculations and Satellite Retrievals. ADIENT/APPRaise CP2 Technical Report, DRAFT V2. Retrieved from: <http://www.reading.ac.uk/adiant/refractiveindices.html>.  
15
- Holben, B. N., Eck, T. F., Slutsker, I., Tanre, D., Buis, J. P., Setzer, A., Vermote, E., Reagan, J. A., Kaufman, Y. J., Nakajima, T., Lavenu, F., Jankowiak, I. and Smirnov, A.: AERONET - A federated instrument network and data archive for aerosol characterization, *Remote Sensing of Environment*, 66(1), 1–16, doi:10.1016/S0034-4257(98)00031-5, 1998.
- 20 Houyoux, M. R., Vukovich, J. M., Coats, C. J., Jr., Wheeler, N. J. M. and Kasibhatla, P. S.: Emission inventory development and processing for the Seasonal Model for Regional Air Quality (SMRAQ) project, *J. Geophys. Res.*, 105(D7), 9079–9090, doi:10.1029/1999JD900975, 2000.
- Hu, X., Waller, L. A., Lyapustin, A., Wang, Y. and Liu, Y.: 10-year spatial and temporal trends of  
25 PM<sub>2.5</sub> concentrations in the southeastern US estimated using high-resolution satellite data, *Atmos. Chem. Phys.*, 14(12), 6301–6314, doi:10.5194/acp-14-6301-2014, 2014.
- Jerrett, M., Turner, M. C., Beckerman, B. S., Pope, C. A., van Donkelaar, A., Martin, R. V., Serre, M., Crouse, D., Gapstur, S. M., Krewski, D., Diver, W. R., Coogan, P. F., Thurston, G. D. and Burnett, R. T.: Comparing the Health Effects of Ambient Particulate Matter Estimated  
30 Using Ground-Based versus Remote Sensing Exposure Estimates, *EHP*, 125(4), 1–8, doi:10.1289/EHP575, 2017.



- Jimenez, J. L., Canagaratna, M. R., Donahue, N. M., Prevot, A. S. H., Zhang, Q., Kroll, J. H., DeCarlo, P. F., Allan, J. D., Coe, H., Ng, N. L., Aiken, A. C., Docherty, K. S., Ulbrich, I. M., Grieshop, A. P., Robinson, A. L., Duplissy, J., Smith, J. D., Wilson, K. R., Lanz, V. A., Hueglin, C., Sun, Y. L., Tian, J., Laaksonen, A., Raatikainen, T., Rautiainen, J., Vaattovaara, P., Ehn, M., Kulmala, M., Tomlinson, J. M., Collins, D. R., Cubison, M. J., E., Dunlea, J., Huffman, J. A., Onasch, T. B., Alfarra, M. R., Williams, P. I., Bower, K., Kondo, Y., Schneider, J., Drewnick, F., Borrmann, S., Weimer, S., Demerjian, K., Salcedo, D., Cottrell, L., Griffin, R., Takami, A., Miyoshi, T., Hatakeyama, S., Shimono, A., Sun, J. Y., Zhang, Y. M., Dzepina, K., Kimmel, J. R., Sueper, D., Jayne, J. T., Herndon, S. C., Trimborn, A. M., Williams, L. R., Wood, E. C., Middlebrook, A. M., Kolb, C. E., Baltensperger, U. and Worsnop, D. R.: Evolution of Organic Aerosols in the Atmosphere, *Science*, 326(5959), 1525–1529, doi:10.1126/science.1180353, 2009.
- Kanakidou, M., Seinfeld, J. H., Pandis, S. N., Barnes, I., Dentener, F. J., Facchini, M. C., Van Dingenen, R., Ervens, B., Nenes, A., Nielsen, C. J., Swietlicki, E., Putaud, J. P., Balkanski, Y., Fuzzi, S., Horth, J., Moortgat, G. K., Winterhalter, R., Myhre, C. E. L., Tsigaridis, K., Vignati, E., Stephanou, E. G., and Wilson, J.: Organic aerosol and global climate modelling: a review, *Atmos. Chem. Phys.*, 5, 1053-1123, <https://doi.org/10.5194/acp-5-1053-2005>, 2005.
- Kloog, I., Chudnovsky, A. A., Just, A. C., Nordio, F., Koutrakis, P., Coull, B. A., Lyapustin, A., Wang, Y. and Schwartz, J.: A new hybrid spatio-temporal model for estimating daily multi-year PM<sub>2.5</sub> concentrations across northeastern USA using high resolution aerosol optical depth data, *Atmospheric Environment*, 95, 581–590, doi:10.1016/j.atmosenv.2014.07.014, 2014.
- Koehler, K. A., Kreidenweis, S. M., DeMott, P. J., Prenni, A. J., Carrico, C. M., Ervens, B., and Feingold, G.: Water activity and activation diameters from hygroscopicity data - Part II: Application to organic species, *Atmos. Chem. Phys.*, 6, 795-809, <https://doi.org/10.5194/acp-6-795-2006>, 2006.
- Laden, F., Schwartz, J., Speizer, F. E. and Dockery, D. W.: Reduction in Fine Particulate Air Pollution and Mortality, *Am J Respir Crit Care Med*, 173(6), 667–672, doi:10.1164/rccm.200503-443OC, 2006.



- Latimer, R. N. C., and R. V. Martin, Interpretation of Measured Aerosol Mass Scattering Efficiency Over North America Using a Chemical Transport Model, *Atmos. Chem. Phys. Discuss.*, 2018, doi:10.5194/acp-2018-459, 2018.
- 5 Lee, H. J., Chatfield, R. B. and Strawa, A. W.: Enhancing the Applicability of Satellite Remote Sensing for PM<sub>2.5</sub> Estimation Using MODIS Deep Blue AOD and Land Use Regression in California, United States, *Environ. Sci. Technol.*, 50(12), 6546-6555, doi:10.1021/acs.est.6b01438, 2016.
- 10 Levy, R. C., S. Mattoo, V. Sawyer, Y. Shi, P. R. Colarco, A. I. Lyapustin, Y. Wang, and L. A. Remer, Exploring systematic offsets between aerosol products from the two MODIS sensors, *Atmos. Meas. Tech.*, 11(7), 4073–4092, doi:10.5194/amt-11-4073-2018, 2018.
- Lim, S. S. et al., A comparative risk assessment of burden of disease and injury attributable to 67 risk factors and risk factor clusters in 21 regions, 1990–2010: a systematic analysis for the Global Burden of Disease Study 2010, *The Lancet*, 380(9859), 2224–2260, doi:10.1016/S0140-6736(12)61766-8, 2012.
- 15 Lyapustin, A., Martonchik, J., Wang, Y., Laszlo, I. and Korkin, S.: Multiangle implementation of atmospheric correction (MAIAC): 1. Radiative transfer basis and look-up tables, *Journal of Geophysical Research: Atmospheres* (1984–2012), 116(D3), D03210, doi:10.1029/2010JD014985, 2011.
- 20 Lyapustin, A. I., Wang, Y., Laszlo, I., Hilker, T., G Hall, F., Sellers, P. J., Tucker, C. J. and Korkin, S. V.: Multi-angle implementation of atmospheric correction for MODIS (MAIAC): 3. Atmospheric correction, *Remote Sensing of Environment*, 127, 385–393, 2012.
- Lyapustin, A., Wang, Y., Korkin, S., and Huang, D.: MODIS Collection 6 MAIAC Algorithm, *Atmos. Meas. Tech. Discuss.*, <https://doi.org/10.5194/amt-2018-141>, in review, 2018.
- 25 Ming, Y., Ramaswamy, V., Ginoux, P. A. and Horowitz, L. H.: Direct radiative forcing of anthropogenic organic aerosol, *J. Geophys. Res.*, 110(D20), 1097–12, doi:10.1029/2004JD005573, 2005.
- 30 Mishchenko, M. I., J. M. Dlugach, E. G. Yanovitskij, and N. T. Zakharova, Bidirectional reflectance of flat, optically thick particulate layers: an efficient radiative transfer solution and applications to snow and soil surfaces, *Journal of Quantitative Spectroscopy and Radiative Transfer*, 63(2), 409–432, doi:[https://doi.org/10.1016/S0022-4073\(99\)00028-X](https://doi.org/10.1016/S0022-4073(99)00028-X), 1999.



- Moise, T., Flores, J. M. and Rudich, Y.: Optical Properties of Secondary Organic Aerosols and Their Changes by Chemical Processes, *Chem. Rev.*, 115(10), 4400–4439, doi:10.1021/cr5005259, 2015.
- 5 Park, S.-K., Marmur, A., Kim, S. B., Tian, D., Hu, Y., McMurry, P. H. and Russell, A. G.: Evaluation of Fine Particle Number Concentrations in CMAQ, *Aerosol Science and Technology*, 40(11), 985–996, doi:10.1080/02786820600907353, 2006.
- Peng, R. D., Bell, M. L., Geyh, A. S., McDermott, A., Zeger, S. L., Samet, J. M. and Dominici, F.: Emergency Admissions for Cardiovascular and Respiratory Diseases and the Chemical Composition of Fine Particle Air Pollution, *EHP*, 117(6), 957–963, 2009.
- 10 Petters, M. D. and Kreidenweis, S. M.: A single parameter representation of hygroscopic growth and cloud condensation nucleus activity, *Atmos. Chem. Phys.*, 7(8), 1961–1971, doi:10.5194/acp-7-1961-2007, 2007.
- Pierce, T., C. Geron, G. Pouliot, E. Kinnee, and J. Vukovich: Integration of the Biogenic Emissions Inventory System (BEIS3) into the Community Multiscale Air Quality (CMAQ) Modeling System, Proceedings of the AMS 4th Urban Environment Symposium, Norfolk, Virginia, 15 20–23 May, 2002.
- Raffuse, S. M., Pryden, D. A., Sullivan, D. C., Larkin, N. K., Strand, T., & Solomon, R.: SMARTFIRE algorithm description. Paper prepared for the U.S. Environmental Protection Agency, Research Triangle Park, NC, by Sonoma Technology, Inc., Petaluma, CA, and the U.S. Forest Service, AirFire Team, Pacific Northwest Research Laboratory, 20 Seattle, WA STI-905517-3719, October, 2009.
- Sarangi, B., Aggarwal, S. G., Sinha, D. and Gupta, P. K.: Aerosol effective density measurement using scanning mobility particle sizer and quartz crystal microbalance with the estimation of involved uncertainty, *Atmos. Meas. Tech.*, 9(3), 859–875, doi:10.5194/amt-9-859-2016, 25 2016.
- Shaddick, G., Thomas, M. L., Green, A., Brauer, M., van Donkelaar, A., Burnett, R., Chang, H. H., Cohen, A., Dingenen, R. V., Dora, C., Gumy, S., Liu, Y., Martin, R., Waller, L. A., West, J., Zidek, J. V. and Prüss-Ustün, A.: Data integration model for air quality: a hierarchical approach to the global estimation of exposures to ambient air pollution, *J. R. Stat. Soc. C*, 30 67(1), 231–253, doi:10.1111/rssc.12227, 2017.



- Shi, L., Zanutti, A., Kloog, I., Coull, B. A., Koutrakis, P., Melly, S. J. and Schwartz, J. D.: Low-Concentration PM<sub>2.5</sub> and Mortality: Estimating Acute and Chronic Effects in a Population-Based Study, *EHP*, 124(1), 1–30, doi:10.1289/ehp.1409111, 2015.
- Snider, G. et al. (2015), SPARTAN: a global network to evaluate and enhance satellite-based estimates of ground-level particulate matter for global health applications, *Atmos. Meas. Tech.*, 8(1), 505–521, doi:10.5194/amt-8-505-2015.
- Snider, G., Weagle, C. L., Murdymootoo, K. K., Ring, A., Ritchie, Y., Stone, E., Walsh, A., Akoshile, C., Anh, N. X., Balasubramanian, R., Brook, J., Qonitan, F. D., Dong, J., Griffith, D., He, K., Holben, B. N., Kahn, R., Lagrosas, N., Lestari, P., Ma, Z., Misra, A., Norford, L. K., Quel, E. J., Salam, A., Schichtel, B., Segev, L., Tripathi, S., Wang, C., Yu, C., Zhang, Q., Zhang, Y., Brauer, M., Cohen, A., Gibson, M. D., Liu, Y., Martins, J. V., Rudich, Y. and Martin, R. V.: Variation in global chemical composition of PM<sub>2.5</sub>: emerging results from SPARTAN, *Atmos. Chem. Phys.*, 16(15), 9629–9653, doi:10.5194/acp-16-9629-2016, 2016.
- Stanier, C. O., Khlystov, A. Y. and Pandis, S. N.: Ambient aerosol size distributions and number concentrations measured during the Pittsburgh Air Quality Study (PAQS), *Atmospheric Environment*, 38(20), 3275–3284, doi:10.1016/j.atmosenv.2004.03.020, 2004.
- Superczynski, S. D., Kondragunta, S. and Lyapustin, A. I.: Evaluation of the multi-angle implementation of atmospheric correction (MAIAC) aerosol algorithm through intercomparison with VIIRS aerosol products and AERONET, *J. Geophys. Res. Atmos.*, 122(5), 3005–3022, doi:10.1002/2016JD025720, 2017.
- Toth, T. D., Zhang, J., Campbell, J. R., Hyer, E. J., Reid, J. S., Shi, Y. and Westphal, D. L.: Impact of data quality and surface-to-column representativeness on the PM<sub>2.5</sub>/satellite AOD relationship for the contiguous United States, *Atmos. Chem. Phys.*, 14(12), 6049–6062, doi:10.5194/acp-14-6049-2014, 2014.
- US EPA, MOVES2014a: Latest version of Motor Vehicle Emission Simulator (MOVES): <https://www.epa.gov/moves/moves2014a-latest-version-motor-vehicle-emission-simulator-moves>, last accessed in April 2018.
- van Donkelaar, A., Martin, R. V. and Park, R. J.: Estimating ground-level PM<sub>2.5</sub> using aerosol optical depth determined from satellite remote sensing, *J. Geophys. Res.*, 111(D21), D21201–10, doi:10.1029/2005JD006996, 2006.





- van Donkelaar, A., Martin, R. V., Brauer, M., Kahn, R., Levy, R., Verduzco, C. and Villeneuve, P. J.: Global Estimates of Ambient Fine Particulate Matter Concentrations from Satellite-Based Aerosol Optical Depth: Development and Application, *EHP*, 118(6), 847–855, doi:10.1289/ehp.0901623, 2010.
- 5 van Donkelaar, A., Martin, R. V., Pasch, A. N., Szykman, J. J., Zhang, L., Wang, Y. X. and Chen, D.: Improving the Accuracy of Daily Satellite-Derived Ground-Level Fine Aerosol Concentration Estimates for North America, *Environ. Sci. Technol.*, 46(21), 11971–11978, doi:10.1021/es3025319, 2012.
- van Donkelaar, A., Martin, R. V., Spurr, R. J. D., Drury, E., Remer, L. A., Levy, R. C. and Wang, J.: Optimal estimation for global ground-level fine particulate matter concentrations, *J. Geophys. Res. Atmos.*, 118(11), 5621–5636, doi:10.1002/jgrd.50479, 2013.
- 10 van Donkelaar, A., R. V. Martin, R. J. D. Spurr, and R. T. Burnett, High-Resolution Satellite-Derived PM<sub>2.5</sub> from Optimal Estimation and Geographically Weighted Regression over North America, *Environ. Sci. Technol.*, 49(17), 10482–10491, doi:10.1021/acs.est.5b02076, 2015.
- 15 van Donkelaar, A., Martin, R. V., Brauer, M., Hsu, N. C., Kahn, R. A., Levy, R. C., Lyapustin, A., Sayer, A. M. and Winker, D. M.: Global Estimates of Fine Particulate Matter using a Combined Geophysical-Statistical Method with Information from Satellites, Models, and Monitors, *Environ. Sci. Technol.*, 50(7), 3762–3772, doi:10.1021/acs.est.5b05833, 2016.
- 20 Zhang, Y., Vijayaraghavan, K., Wen, X.-Y., Snell, H. E. and Jacobson, M. Z.: Probing into regional ozone and particulate matter pollution in the United States: 1. A 1 year CMAQ simulation and evaluation using surface and satellite data, *J. Geophys. Res.*, 114(D22), D22304, doi:10.1029/2009JD011898, 2009.



## Tables

*Table 1:* Optical properties used to calculate AOD<sub>CMAQ</sub> in FlexAOD. Values in square brackets represent the range of uncertainties in given parameter, which are used for the sensitivity runs in FlexAOD to quantify their impacts on the satellite-derived PM<sub>2.5</sub>.

5

	Sulfate	OC	BC	Sea Salt	Dust
Modal radius <sup>a</sup> ( $r_0$ , $\mu\text{m}$ )	0.11 <sup>b</sup> [0.05 <sup>c</sup> ~ 0.15]	0.09 <sup>b</sup> [0.02 <sup>d</sup> ~ 0.12 <sup>e</sup> ]	0.02 <sup>b</sup>	0.40 <sup>b</sup>	
Geometric standard deviation <sup>a</sup> ( $\sigma$ , g)	1.6 <sup>b</sup>	1.6 <sup>b</sup>	1.6 <sup>b</sup>	1.5 <sup>b</sup>	
Aerosol density ( $\rho$ , $\text{g}/\text{cm}^3$ )	1.7 <sup>b</sup> [1.65, 1.83] <sup>e</sup>	1.3 <sup>b</sup> [1.2, 1.78] <sup>f</sup>	1.0 <sup>b</sup>	2.2 <sup>b</sup>	
Refractive Index ( $m$ ) at 550 nm	1.53 <sup>g</sup> [1.43 <sup>d</sup> , 1.6 <sup>e</sup> ] - $i$ 0.006 <sup>g</sup>	1.53 <sup>g</sup> [1.37, 1.65] <sup>h</sup> - $i$ 0.008	1.75 - $i$ 0.44 <sup>g</sup>	1.5 - $i$ 10 <sup>-8</sup> <sup>g</sup>	1.53 - $i$ 0.0055 <sup>g</sup>
Hygroscopic growth factor ( $f$ ) at RH = 90%	1.77 [1.58, 1.96] <sup>i</sup>	1.24 <sup>i</sup> [1.0 <sup>k</sup> , 1.41] <sup>j</sup>	1.4 <sup>d</sup>	2.4 <sup>d</sup>	1.0 <sup>d</sup>
	1.8 <sup>d</sup>	1.6 <sup>d</sup>	1.4 <sup>d</sup>	2.4 <sup>d</sup>	1.0 <sup>d</sup>
	5.1 <sup>k</sup>	1.0 <sup>k</sup>	1.4 <sup>d</sup>	2.4 <sup>d</sup>	1.0 <sup>d</sup>

Note:

- a. Assuming log-normal distribution for aerosol species except for dust. The effective radius is calculated as:  $r_e = r_0 e^{\left(\frac{5}{2} \ln^2 \sigma_g\right)}$ .
- b. Drury et al. (2010).
- 10 c. Highwood et al. (2009).
- d. Chin et al. (2002)
- e. Sarangi et al., (2016)
- f. Park et al., (2006)
- 15 g. OPAC (Hess et al., 1998)
- h. Moise et al., (2015)
- i.  $\kappa$  parameter (Petters and Kreidenweis, 2007). The hygroscopic factor ( $f$ ) is calculated as:  $f(\text{RH}) = \left(1 + \kappa \frac{\text{RH}}{100 - \text{RH}}\right)^{1/3}$  following Snider et al. (2016), where  $\kappa = 0.53$  in the default run,  $\kappa = 0.33$  for the low end,  $\kappa = 0.72$  for the high end.
- 20 j. Calculated from  $\kappa$  parameter equation, where  $\kappa = 0.1$  in the default run,  $\kappa = 0.2$  for the high end (Jimenez et al., 2009; Duplissy et al., 2011).
- k. Empirical hygroscopic growth factors used by the revised IMPROVE algorithm (Hand and Malm, 2006) to calculate light extinction (<http://vista.cira.colostate.edu/Improve/the-improve-algorithm/>). The revised IMPROVE algorithm assumes no hygroscopic growth for OC.



### Figures

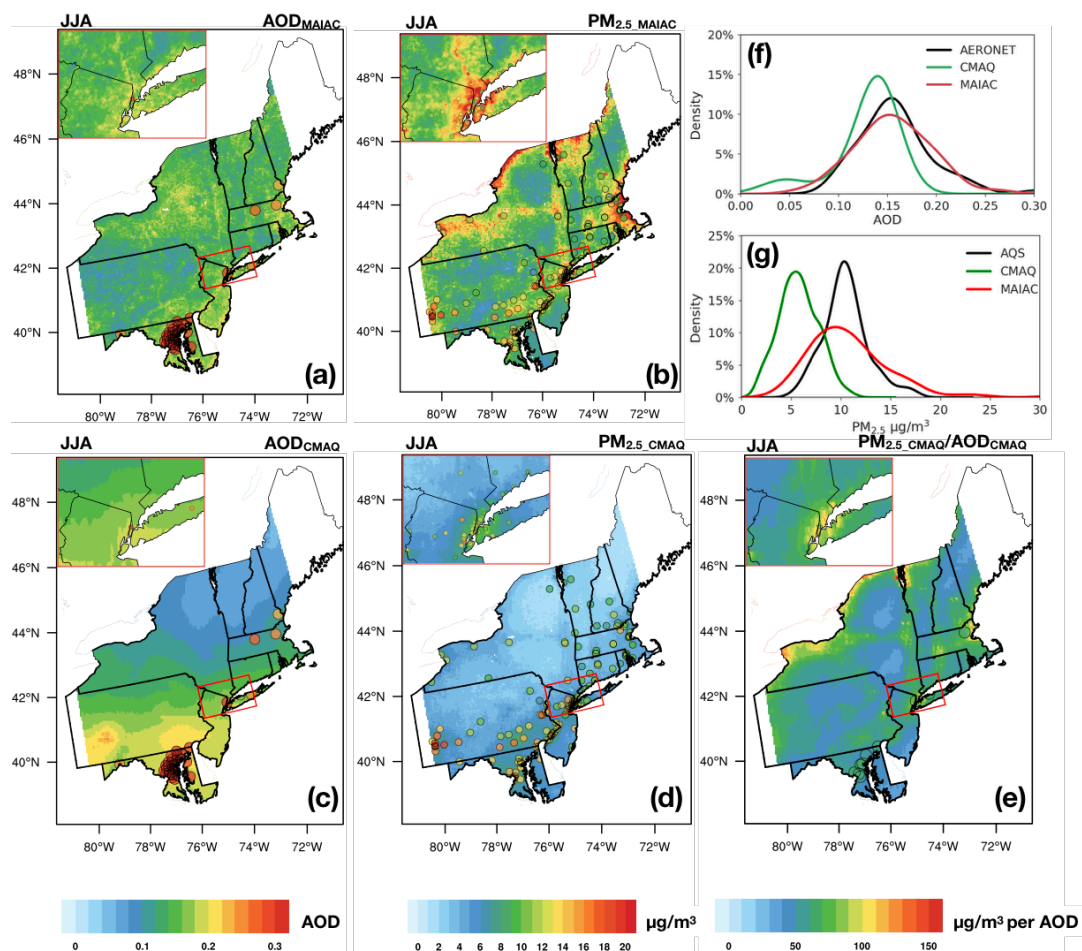


Figure 1 Summertime (JJA) average: (a) MAIAC AOD ( $AOD_{MAIAC}$ ); (b) satellite-derived  $PM_{2.5}$  ( $PM_{2.5\_MAIAC}$ ); (c) CMAQ model AOD ( $AOD_{CMAQ}$ ); (d) CMAQ model  $PM_{2.5}$  ( $PM_{2.5\_CMAQ}$ ); (e) CMAQ modeled  $PM_{2.5}/AOD$  ( $PM_{2.5\_CMAQ}/AOD_{CMAQ}$ ) ratio overlaid with ground-based observations (AERONET, AQS, co-located AERONET and AQS sites) over the Northeast USA with zoom-in maps over the New York City region in the upper left corner. (f) Density plot of AOD showing the distribution of MAIAC, CMAQ and AERONET observed AOD sampled at AERONET sites. (g) Density plot of  $PM_{2.5}$  showing the distribution of satellite-derived, CMAQ and AQS observed  $PM_{2.5}$  sampled at AQS sites.

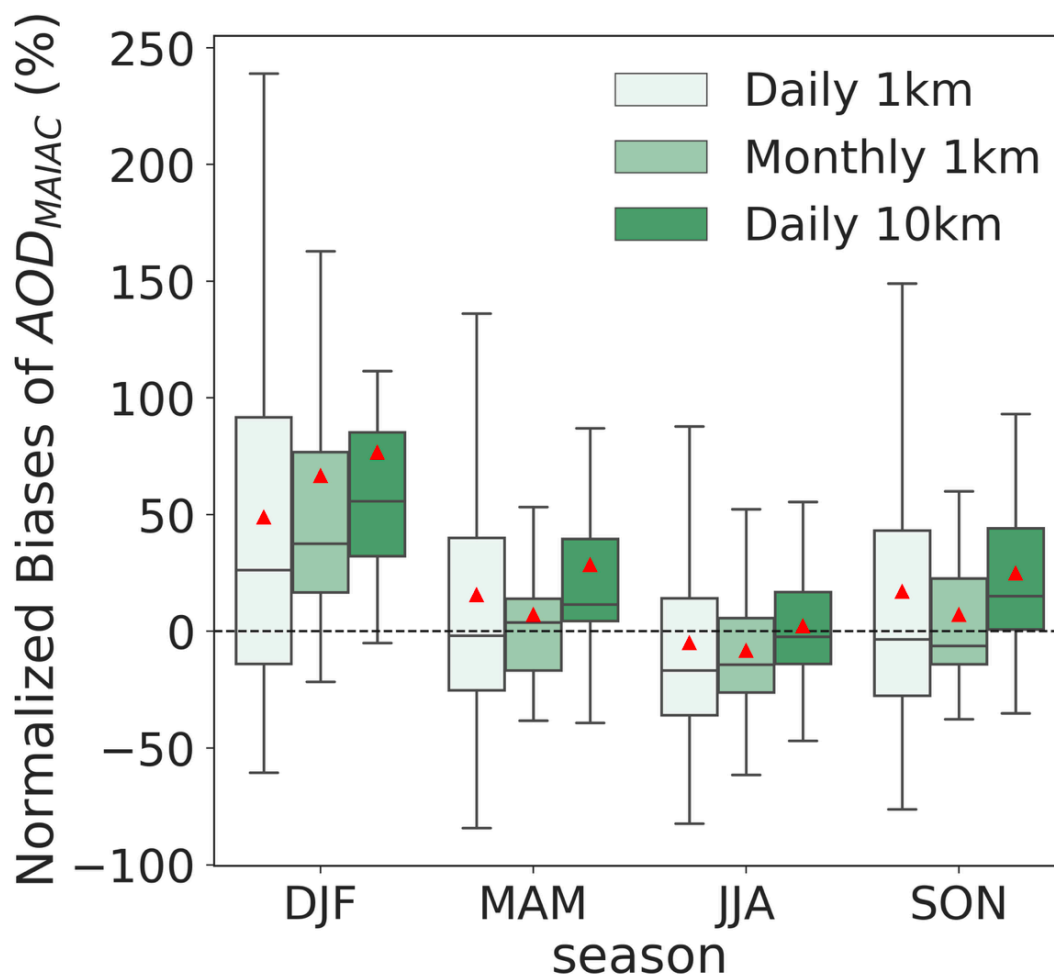


Figure 2 Distribution of normalized biases of  $AOD_{MAIAC}$  evaluated at 52 AERONET (including DRAGON, only available for JJA) sites in four seasons of 2011 over the Northeast USA using daily MAIAC AOD at 1 km resolution, 10 km resolution, and monthly average MAIAC AOD composite (only including days when both satellite and AERONET measurements are available) at 1 km resolution. The box shows the quantile range (IQR) while the whiskers extend to show the rest of the distribution with outliers (points that are either  $1.5 \times IQR$  or more above the third quartile or below the first quartile) removed. The red triangles show the seasonal mean normalized biases. Note that the normalized bias is an asymmetric metric, where model overestimates are unbounded whereas model underestimates are bounded by  $-100\%$ , therefore the mean of normalized biases is typically higher than the median of the normalized biases.

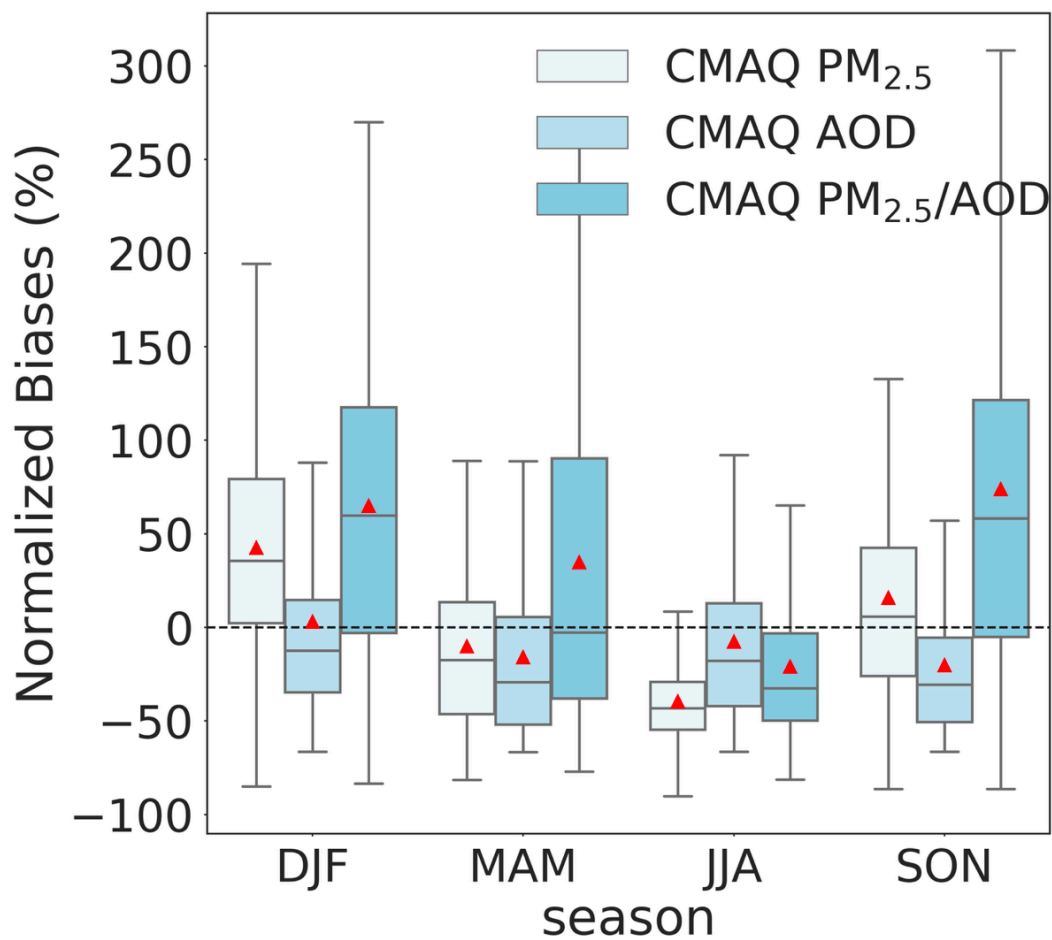


Figure 3 As in Figure 2 but for daily  $PM_{2.5\_CMAQ}$ ,  $AOD_{CMAQ}$ , and  $PM_{2.5\_CMAQ}/AOD_{CMAQ}$  in each season of 2011 evaluated at 11 co-located AQS-AERONET sites over the Northeast USA.

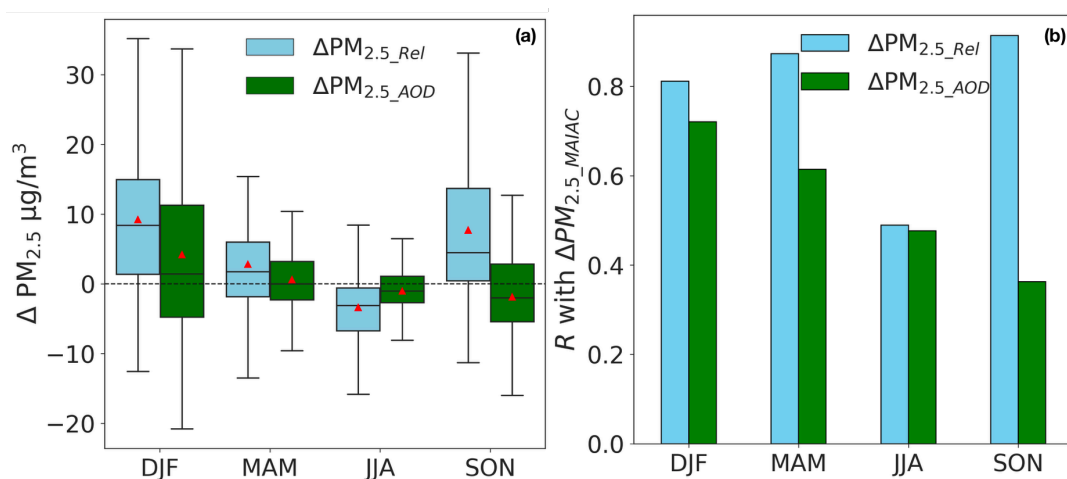


Figure 4 (a) Box plots comparing the distribution of biases in daily  $\text{PM}_{2.5\_MAIAC}$  due to observational uncertainties in  $\text{AOD}_{MAIAC}$  (green,  $\Delta \text{PM}_{2.5\_AOD}$ ) versus model uncertainties in  $\text{PM}_{2.5\_CMAQ}/\text{AOD}_{CMAQ}$  (blue,  $\Delta \text{PM}_{2.5\_Rel}$ ), evaluated consistently at 11 co-located AQS-AERONET sites over the Northeast USA. (b) Pearson correlation coefficient between the biases in daily satellite-derived  $\text{PM}_{2.5}$  ( $\Delta \text{PM}_{2.5\_MAIAC}$ , evaluated with AQS observations) and the biases in  $\text{PM}_{2.5\_AOD}$  attributed to observational uncertainties in  $\text{AOD}_{MAIAC}$  ( $\Delta \text{PM}_{2.5\_AOD}$ ) versus model uncertainties in  $\text{PM}_{2.5\_CMAQ}/\text{AOD}_{CMAQ}$  ( $\Delta \text{PM}_{2.5\_Rel}$ ).  $\Delta \text{PM}_{2.5\_AOD}$  is calculated by multiplying the biases of  $\text{AOD}_{MAIAC}$  with daily modeled  $\text{PM}_{2.5}/\text{AOD}$  relationships (Eq. (8)).  $\Delta \text{PM}_{2.5\_Rel}$  is calculated by multiplying the modeled  $\text{PM}_{2.5}/\text{AOD}$  biases with daily  $\text{AOD}_{MAIAC}$  (Eq. (9)). The red triangles show the seasonal mean biases.

15

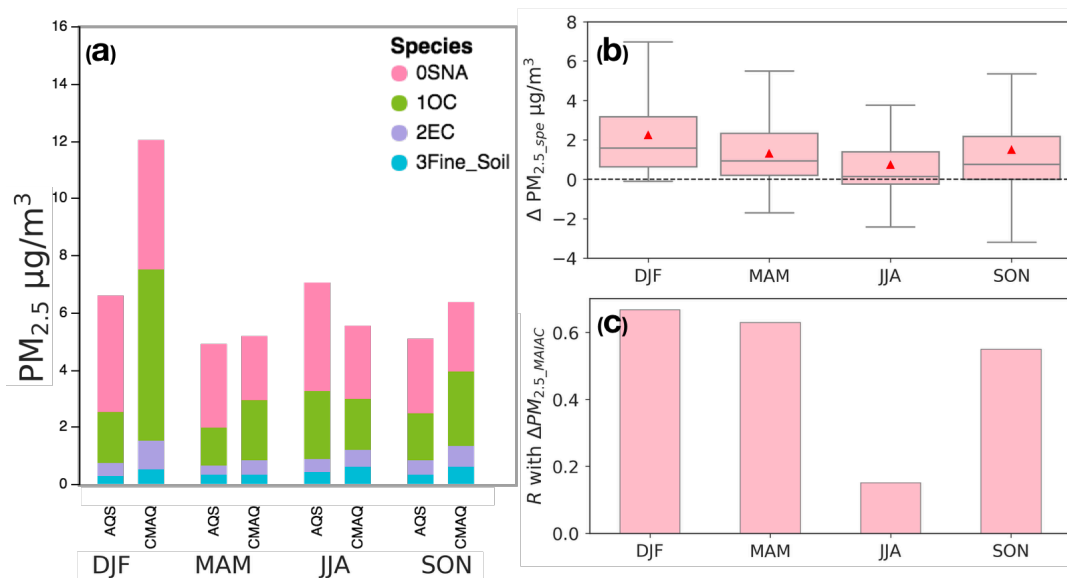


Figure 5 (a) Seasonal average  $PM_{2.5}$  speciation from CMAQ vs. AQS observations in 2011 evaluated at 54 CSN and IMPROVE sites. (b) Box plots showing the distribution of estimated biases of daily satellite-derived  $PM_{2.5}$  due to model biases in  $PM_{2.5}$  speciation ( $\Delta PM_{2.5\_spe}$ ) by season for 2011. Red triangles show the seasonal mean biases. (c) Pearson correlation coefficient between the biases in  $PM_{2.5\_MAIAC}$  ( $\Delta PM_{2.5\_MAIAC}$ ) and  $\Delta PM_{2.5\_spe}$ .

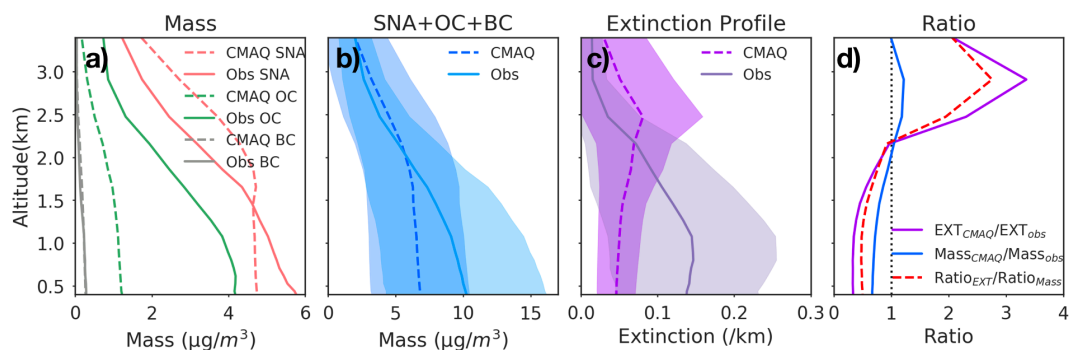


Figure 6 Campaign-mean vertical profiles of: (a) aerosol composition, (b) total mass (SNA+OC+BC), and (c) extinction from CMAQ vs. observations from the DISCOVER-AQ 2011 Baltimore-Washington D.C. campaign. (d) Campaign-mean vertical profile of the model-to-observation ratio of extinction ( $\text{Ratio}_{\text{EXT}}$ ), total aerosol mass ( $\text{Ratio}_{\text{Mass}}$ ) and  $\text{Ratio}_{\text{EXT}}/\text{Ratio}_{\text{Mass}}$ . Aircraft observations are first aggregated to match model layers, and corresponding model values are sampled concurrently with the time of observations. CMAQ modeled extinction is estimated with FlexAOD using the default parameters in Table 1. The shading in (b) and (c) shows the standard deviation of the day-to-day variability.



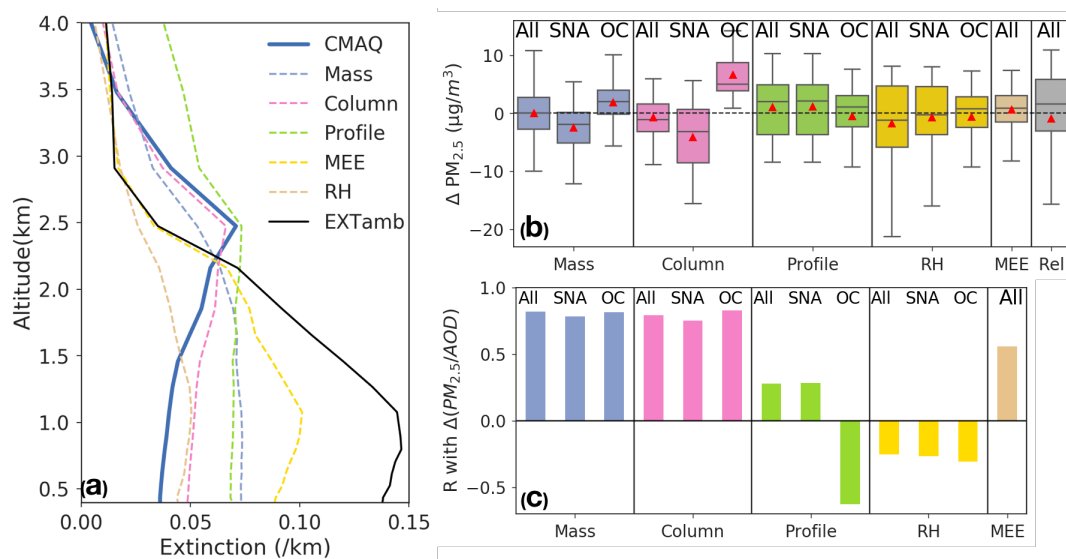


Figure 7 (a) Campaign-mean vertical profiles of extinction calculated from CMAQ speciated aerosol fields using FlexAOD, and that calculated by replacing modeled speciated aerosol mass (Mass), total column mass (Column), vertical profile shape (Profile), total mass extinction efficiency (MEE), relative humidity (RH) with that observed from DISCOVER-AQ 2011 Baltimore-Washington D.C. campaign. EXT<sub>amb</sub> is the aircraft observed vertical extinction profile. (b) Box plots showing the distribution of biases of PM<sub>2.5\_MAIAC</sub> attributed to each factor shown in (a), and the biases of PM<sub>2.5\_MAIAC</sub> attributed to modeled PM<sub>2.5/AOD</sub> (Rel). Red triangles show the mean biases. (c) Pearson correlation coefficient between the biases in modeled PM<sub>2.5/AOD</sub> relationships and the biases in modeled PM<sub>2.5/AOD</sub> attributed to individual factors shown in (b).

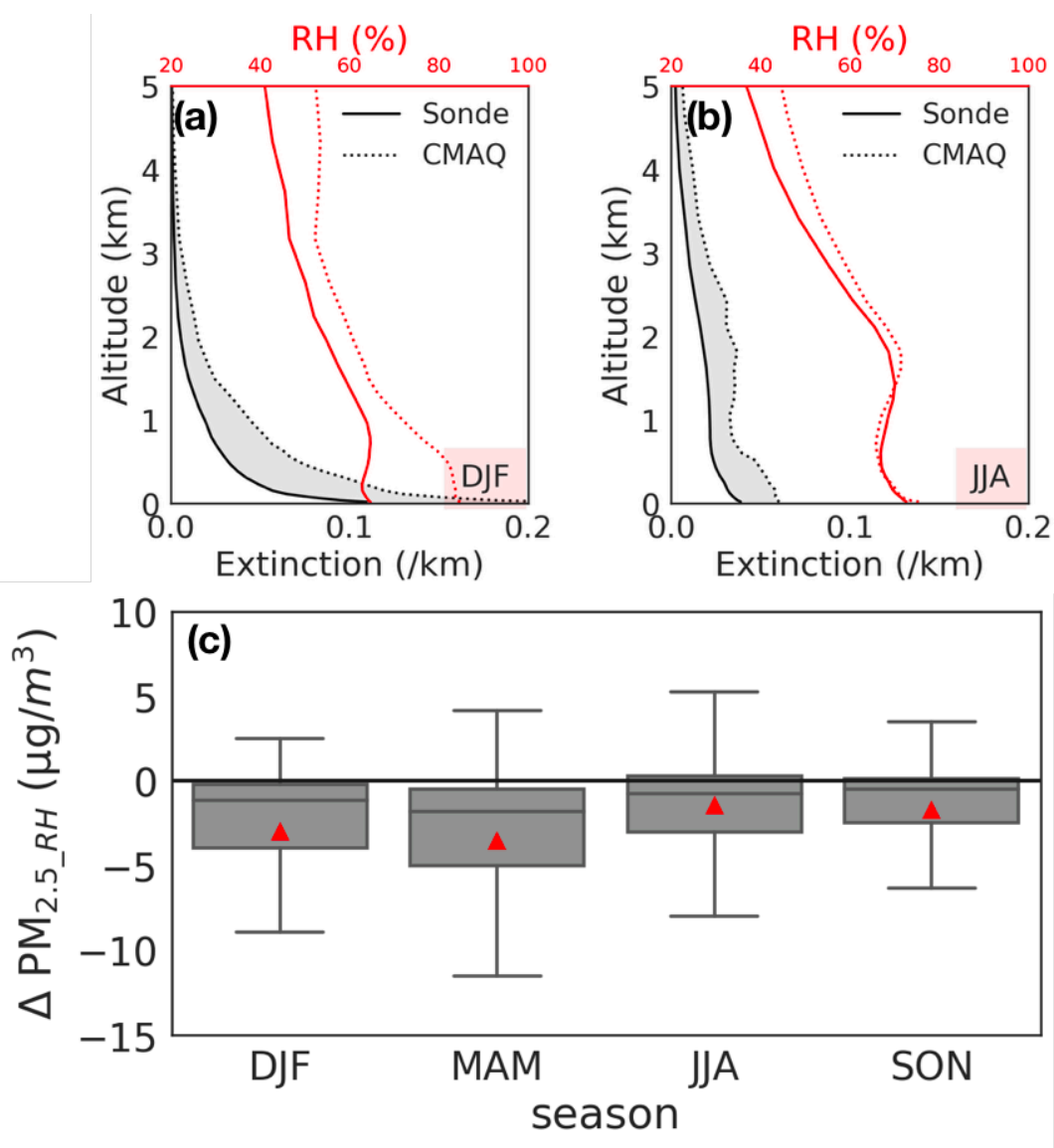


Figure 8 (a) DJF and JJA average vertical profiles of the CMAQ modeled vs. observed RH at 6 atmospheric soundings over the Northeast USA, and the modeled extinction vs. that calculated by replacing modeled RH with observed values. The gray area shows the difference in extinction two profiles, with the total area being the difference in AOD. (b) Box plots showing the impacts of model bias of RH on the derived  $PM_{2.5\_MAIAC}$  ( $\Delta PM_{2.5\_RH}$ ) in four seasons of 2011, which are calculated by comparing the  $PM_{2.5\_MAIAC}$  minus the one calculated using observed RH. Red triangles show the mean biases.

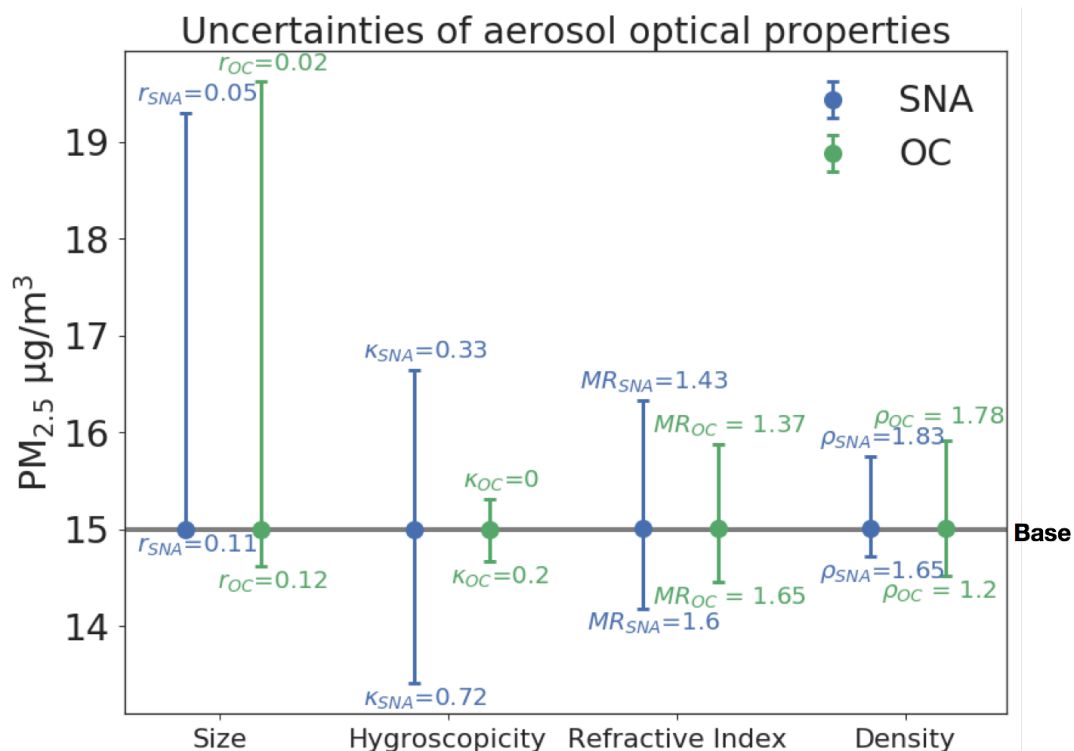


Figure 9 Uncertainties in annual average satellite-derived  $PM_{2.5\_MAIAC}$  due to uncertainties of size distribution, hygroscopicity, refractive index and aerosol species density of sulfate-nitrate-ammonium (SNA; blue) and organic carbon (OC; green) sampled over AQS sites. The circle shows the annual average satellite-derived  $PM_{2.5\_MAIAC}$  using the default parameters to calculate  $AOD_{CMAQ}$  in FlexAOD (Table 1). The error bars represent the range of  $PM_{2.5\_MAIAC}$  using different values for each parameter. The labels indicate the corresponding minimum or maximum parameter values that produce the range shown in  $PM_{2.5\_MAIAC}$ . The horizontal line at  $15 \mu\text{g}/\text{m}^3$  indicates the annual average  $PM_{2.5\_MAIAC}$  calculated using default values for each aerosol optical property in the base FlexAOD.